FINAL TECHNICAL REPORT

Federal Agency and Organization Element to Which Report is Submitted
Department of Energy - National Energy Technology Laboratory (DOE – NETL)
Organization Element: NETL - HBCU/UCR

Federal Grant or Other Identifying Number Assigned by Agency
DOE Contract No.: DE-FE0026325

Project Title
Novel High Temperature Carbide and Boride Ceramics for Direct Power Extraction Electrode Applications

PD/PI Name, Title and Contact Information (e-mail address and phone number)
Zhe Cheng, Associate Professor, Florida International University
10555 W. Flagler ST EC3441, Miami, FL 33174
Email: zhcheng@fiu.edu ; Phone: 305-348-1973

Name of Submitting Official, Title, and Contact Information
Same as PI

Submission Date
12/12/2020

DUNS Number
0712988140000

Recipient Organization (Name and Address)
Florida International University
11200 SW 8th Street, MARC 430, Miami, FL 33199-0001

Project/Grant Period (Start Date, End Date)
10/01/2015 to 09/30/2020 (**no cost extension to 09/30/2020 approved on 07/25/2019**)

Report Preparer
Zhe Cheng (PI)

Signature of Submitting Official

ABSTRACT
The current project aims to develop new carbide and boride ceramic materials that incorporate different metal elements (e.g., $(Hf_{1-x}Zr_x)B_2$, also called ceramic solid solutions) and understand the fundamental composition-processing-structure-property relationships for such materials. Specifically, nano powders and related nano-composites for selected mixed metal carbide and boride materials are synthesized from nano-scale mixed precursors obtained from solution-based processing via heat treatment in inert atmosphere. The obtained fine powders were then consolidated into dense ceramics via a novel flash sintering process. The mechanical properties and thermal oxidation resistance for the obtained materials were evaluated for these materials. It was found that different synthesis routes produced powders with somewhat different characteristics in terms of composition and microstructure, which then led to different properties for the final ceramics. The synthesis and processing methods demonstrated in this study might be adopted for developing other similar high temperature ceramics, while the mixed metal or solid solution ceramic materials obtained from this study might be used as hot electrodes for direction power extraction and other energy-related applications.

<u>Training of Minority Undergraduate and Graduate Students</u>

Over the course of the project, three minority students have been supported as undergraduate and graduate research assistant.

- Mr. **Driany Alfonso**
  US citizen, minority
  Undergraduate research assistant, 12/2015-07/2016
  Transferred to University of Florida in 08/2016
- Mr. **Andres Behrens**
  US citizen, minority
  Graduate research assistant, 05/2016-12/2017
  Graduated with MS from FIU in 08/2018
  Currently patent examiner at United States Patents & Trademark Office (USPTO)
- Mr. **Jose Belisario**
  US citizen, minority student
  Graduate research assistant, 05/2018-12/2019
  Graduated with MS from FIU in 12/2019
  Currently pursuing PhD in Materials Science & Engineering at University of Central Florida (UCF)

All of the above students had made active contributions to this project as well as other research work in the PI's group. The following is a list of publications which the minority students published as the 1st author or contributed to:

1. Cheng, Zhe; Foroughi, Paniz; **<u>Behrens, Andrés</u>**, "Synthesis of high temperature ceramic powders," US Patent 9,919,973.
2. Cheng, Zhe; Foroughi, Paniz; **<u>Behrens, Andrés</u>**. "Synthesis of nanocrystalline TaC powders via single-step high temperature spray pyrolysis from solution precursors," *Ceramics International* (2017), 43(3), 3431-3434. DOI:0.1016/j.ceramint.2016.11.177
3. Mondal, Santanu; Durygin, Andriy; Drozd, Vadym; **<u>Belisario, Jose</u>**; Cheng, Zhe. "Multicomponent bulk metal nitride $(Nb_{1/3}Ta\mathbf{1/3}Ti_{1/3})N_{1-\delta}$ synthesis via reaction flash sintering and characterizations," *Journal of the American Ceramic Society* (2020), 103(9), 4876-4893. DOI:10.1111/jace.17226
4. **<u>Belisario, Jose</u>**; Mondal, Mondal; Khakpour, Iman; Franco Hernandez, Alexander; Durygin, Andriy; Cheng, Zhe. 'Synthesis and flash sintering of $(Hf_{1-x}Zr_x)B_2$ solid solution powders,' *Journal of European Ceramic Society*, Accepted, JECS13774, Manuscript ID JECS-D-20-01945R2 (2021).

Summary of Technical Achievement

The major technical contribution for this project has been summarized by our accepted manuscript, as below.

Synthesis and flash sintering of $(Hf_{1-x}Zr_x)B_2$ solid solution powders

Jose Belisario[1,2] | Santanu Mondal[1,2] | Iman Khakpour[1] | Alexander Franco Hernandez[1] | Andriy Durygin[2] | Zhe Cheng[1,2,*]

[1]*Department of Mechanical and Materials Engineering, Florida International University, Miami, Florida 33174, USA*

[2]*Center for the Study of Matter at Extreme Conditions (CeSMEC), Florida International University, Miami, Florida 33174, USA*

**Corresponding author email: zhcheng@fiu.edu*

Correspondence

Zhe Cheng, Department of Mechanical and Materials Engineering, Florida International University, Miami, Florida 33174, USA, zhcheng@fiu.edu

Funding information

DOE National Energy Technology Laboratory (NETL) Crosscutting Research Technology Program
Grant/Award Number: DE-FE0026325

ABSTRACT

$(Hf_{1-x}Zr_x)B_2$ solid solution powders were synthesized by two methods. First, solution-based processing of $HfCl_4$, $ZrCl_4$, sucrose, and H_3BO_3 was conducted followed by heat treatment in Argon to carry out the carbothermal reduction (CTR) reaction to form the diboride powders. Alternatively, in the so-called borohydride reduction (BHR) method, $HfCl_4$, $ZrCl_4$ and $NaBH_4$ were mixed in an Argon glove box followed by heat treatment in Argon at 700-1500°C. The synthesized powders were characterized by XRD, SEM, TEM, EDS, and TGA, and the influence of different parameters such as starting composition, heat treatment temperature and time on products characteristics were revealed. Both CTR and BHR solid solution powders were then consolidated within ~5 min in a homemade flash sintering (FS) setup. The composition, microstructure, hardness, and thermal-oxidation properties of flash sintered ceramics were characterized, and the implication of this study and directions for future research were discussed.

Keywords: solid solution, borides, ultra-high temperature ceramics, carbothermal reduction (CTR), borohydride reduction (BHR)

1 | INTRODUCTION

Group IV metal (Ti, Zr, Hf) diborides have a combination of properties such as high melting points (>3000°C), high hardness (>20 GPa) and elastic modulus (~480 GPa), high electrical conductivity (~10^7 S/m) and thermal conductivity (60-120 W/m·K) comparable to many metals, and excellent chemical stability[1-3]. Earlier investigations also showed that diborides are resistant to erosion attacks and corrosion, with hafnium diboride (HfB_2, T_m = 3250°C) at the top of the list, followed by zirconium diboride (ZrB_2, T_m = 3246°C). Furthermore, when compared to metal carbides and nitrides, the higher thermal conductivity of diborides offers better thermal shock resistance for high temperature applications. These properties make ZrB_2 and HfB_2 the primary candidates for applications in extreme environments such as wing leading edges and nose tips on hypersonic and atmospheric re-entry vehicles as well as components for rocket propulsion system [4].

However, for hypersonic aerospace flights in the upper atmosphere under low oxygen partial pressure condition, hafnium dioxide (HfO_2) and zirconium dioxide (ZrO_2), as the porous oxidation products of HfB_2 and ZrB_2, may also become nonstoichiometric by forming oxygen vacancies, which would allow significant oxygen ion transport through the oxide layer and result in rapid oxidation of the whole structure [5]. In addition, the relatively low fracture toughness of HfB_2 and ZrB_2 is also a concern when using these ceramics under extreme thermal shock and cycling loading conditions [5].

To overcome these deficiencies (e.g., lower than ideal oxidation resistance and toughness), researchers have tried adding reinforcing phase(s) to form a composite. For example, it is well known that adding SiC to form a ZrB_2-SiC composite improves the oxidation resistance over ZrB_2 by changing the composition of the oxide scale and forming a silica-rich scale [1, 6]. Meanwhile, adding *alloying elements* to form solid solutions is another method to tune materials' composition and optimize for better physical or chemical properties [5-9]. For diborides, solid solutions form among Group IV and V metals. In particular, since the atomic radii differ by <10%, HfB_2 and ZrB_2 form continuous solid solutions with each other and also with TiB_2, NbB_2, and TaB_2 [1]. Some of these solid solutions further display improved properties, like hardness, as compared to the end compositions. For instance, the TiB_2–ZrB_2 solid solution containing 40 mol% ZrB_2 showed the highest hardness of 30.4 GPa when compared to 23 GPa for ZrB_2 and 25 GPa for TiB_2 [1, 10]. In another study, $W_{1-x}Nb_xB_2$ and $W_{1-x}Ta_xB_2$ showed hardness of 40.3 ± 1.6 GPa for 6 at. % Nb and 41.0 ± 1.2 GPa for 8 at. % Ta substitution - both higher than the value of 29.5 ± 1.7 GPa for unsubstituted WB_2 [11].

For this study, two low-cost and facile processes were selected to synthesize (Hf, Zr)B_2 solid solution powders. The first is based on the carbothermal reduction (CTR) reaction, which, in this case, involves the high temperature reaction of metal oxide(s) and boron oxide with carbon as the reducing agent. Unlike the commercial production involving CTR that utilizes coarse mixture of oxides and carbon, in this study, the CTR-based method begins from an aqueous solution of low-cost precursors of hafnium tetrachloride ($HfCl_4$), zirconium tetrachloride ($ZrCl_4$), boron acid (H_3BO_3), and sucrose ($C_{12}H_{22}O_{11}$) as the metals, boron, and carbon sources, respectively. Through processing of the aqueous solution, which involves multiple processes including hydrolysis, condensation, solvent evaporation, and thermal decomposition (or pyrolysis, typically at ~400-800ºC), a nano-scale mixture of $(Hf_{1-x}Zr_x)O_2$ (presumably a solid solution between HfO_2 and ZrO_2 since the two oxides are extremely similar and have high affinity to each other), boron trioxide (B_2O_3), and carbon is obtained. Thereafter, such nano-scale mixtures react at elevated temperature (e.g., 1500°C) through the endothermic CTR reaction to produce the targeted metal diboride(s) as well as carbon monoxide (CO) as a byproduct [1, 5]. Overall, the idealized CTR reaction in this case may be written as:

$$(Hf_{1-x}Zr_x)O_2 + B_2O_3 + 5C = (Hf_{1-x}Zr_x)B_2 + 5CO. \quad (1)$$

It is noted the CTR-based process reported here bears some similarity to a few previous reports such as the one by Wang et al. [12]. However, there are also significant differences: (i) Wang's study targets pure HfB_2 instead of $(Hf_{1-x}Zr_x)B_2$ solid solution powders in this study. (ii) Wang utilized phenolic resin as the carbon precursor and ethanol as the solvent, as opposed to sucrose and water in the current method. (iii) Wang used HfO_2 powder directly and the boron precursor was B_4C, both of which are not soluble in the ethanol solvent, as opposed to all soluble precursors (i.e., $HfCl_4$, $ZrCl_4$, and boric acid) in the current method.

The second method used in this study is based on the reaction between a metal salt and certain alkaline metal borohydride [1, 13, 14], and it may be called the borohydride reduction (BHR) method. In this method, the same low-cost metal precursors (e.g., $HfCl_4$ and $ZrCl_4$) are directly mixed and reacted with metal borohydride such as sodium borohydride ($NaBH_4$) as the reductant as well as the boron precursor. Synthesis of nanocrystalline HfB_2 and ZrB_2 have been successfully conducted at rather low temperature via this method. For instance, Chen et al. reported the synthesis of nanocrystalline HfB_2 at 600°C and ZrB_2 in the temperature range of 500-700 °C using an autoclave [13, 14]. For the current system, the hypothesized overall BHR reaction between $HfCl_4$, $ZrCl_4$, and $NaBH_4$ might be simplified as:

$$(1-x)\ HfCl_4 + x\ ZrCl_4 + 2\ NaBH_4 = (Hf_{1-x}Zr_x)B_2 + 2NaCl + 2HCl + 3H_2 \quad (2)$$

Of course, the detailed reaction process could be more complex than above, given that $NaBH_4$ is not stable at elevated temperature (>500°C) and may decompose and react to form different products/by-products [13, 14].

The $(Hf_{1-x}Zr_x)B_2$ solid solution powders (x = 0.25, 0.5, and 0.75) as well as the two end compositions (x = 0 and 1) obtained from the above two methods were characterized using different techniques. The influence of various synthesis parameters (e.g., starting composition, heat treatment temperature and time) on the phase formation has been investigated.

Apart from powder synthesis, because such diboride materials are mostly used as bulk ceramics, solid solution powders for a particular composition - $Hf_{0.5}Zr_{0.5}B_2$ synthesized by both the CTR-based and BHR methods were further consolidated within ~5 min into dense bulk ceramics using a home-made flash sintering setup. Flash sintering is a type of field assisted sintering technique that applies an electric field (typically DC) to a powder compact and force the electrical current to pass only through the sample [15]. It is often characterized by rapid drop in sample resistance and dramatic increase in current and power dissipation, leading to extremely fast increase in sample temperature and rapid densification (within a few minutes or even seconds) at much lower surrounding temperature than conventional sintering. It should be noted that there have been some earlier studies on the rapid (within one minute) densification of ZrB_2 and HfB_2 powders by the flash spark plasma sintering (FSPS) technique. However, those studies relied on complex and expensive commercial SPS system and involved either a separate 1600°C/20 min pre-sintering step or a 600°C/2h phenolic resin pyrolysis step before the actual FSPS [16, 17]. Finally, the microstructure, properties such as hardness and thermal-oxidation resistance for the flash sintered $(Hf_{0.5}Zr_{0.5})B_2$ samples were investigated, and the inter-relationship between processing, microstructure, and properties are discussed. The potential directions for future research on synthesis and processing of multi-component high temperature ceramic powders including their efficient sintering are also pointed out.

2 | EXPERIMENTAL

2.1 | Synthesis and characterization of hafnium-zirconium diboride solid solution powders

In this study, the recipes, the processing conditions, and the phase information (from XRD) of $(Hf_{1-x}Zr_x)B_2$ solid solution powders synthesized via the CTR-based method are summarized in Table 1. As stated, the metal precursors were hafnium tetrachloride ($HfCl_4$, 98+% metal basis excluding Zr, Zr<2.7%, Alfa Aesar #11834) and zirconium tetrachloride ($ZrCl_4$, 99.5+%, Alfa Aesar #12104), while sucrose ($C_{12}H_{22}O_{11}$, 99.5%, Sigma #S9378) and boric acid (H_3BO_3, 99.99%, +8 Mesh Granular, Alfa Aesar #36771) were the carbon and boron sources, respectively. First, $HfCl_4$ and $ZrCl_4$ were dissolved in separate beakers in deionized (DI) water (typically 0.005 mole of the chloride powder in ~35 g of water) while being magnetically stirred on a hot plate set at ~225°C to form separate clear colorless solutions of hafnium oxychloride ($HfOCl_2$) and zirconium oxychloride ($ZrOCl_2$). The two transparent oxychloride solutions were then mixed together in one beaker. Then, sucrose was dissolved into the mixed solution. Thereafter, H_3BO_3 was dissolved into the mixed solution, while the hotplate was still set at ~225°C. The stir bar was retrieved when the mixed solution became viscous and brown, and the solution was heated continuously with manual stirring by a metal spatula until it was dry. After that, the dried mixture was retrieved and ground with mortar and pestle until powder was obtained.

The dried and ground precursor powders were transferred into a cylindrical graphite crucible (OD = 29.6 mm, ID = 22.0 mm, length = 38.8 mm) with a lid (see Figure S1 in the supporting document) and placed inside a 32.4 mm ID tube furnace and heat treated at elevated temperatures (e.g., 1500°C, see Table 1 for more details) in flowing argon (UHP grade, Airgas) at a flow rate of ~80 cc/min with heating and cooling rate of 5°C/min. In particular, during the heat up at temperature below ~800°C, dehydration and pyrolysis (i.e., thermal decomposition) of the precursors are expected to take place, and low molecular weight species (e.g., water, carbon monoxide, and hydrogen chloride) are removed to produce a uniform (Hf, Zr)O_2-B_2O_3-C nano-scale mixture [5, 18, 19]. To illustrate this, Figure S2 in the supporting document shows TGA-DSC up to 1450°C in Argon for dried precursor from recipe C33 (starting Hf : Zr : B : C molar ratio = 0.5 : 0.5 : 3 : 10). The dried sample loses weight, first quickly and then slowing down as it is heated up to ~700°C. In addition, Figure S3A shows XRD for dried precursor from C33 after a pyrolysis heat treatment

TABLE 1 Summary of starting materials molar ratio, temperature and time for the final CTR heat treatment (in argon), and the resulting phase information (from XRD) for various powder samples targeting $(Hf_{1-x}Zr_x)B_2$ synthesized via the CTR-based method.

Sample ID	Recipe	Starting Hf : Zr : B : C molar ratio [a]	Temp (°C)	Holding time	Actual phase(s) from XRD
C1-1500-60m	C1	1 : 0 : 3 : 10	1500	1 h	HfB_2
C21-1500-60m	C21	0.75 : 0.25 : 3 : 10	1500	1 h	$(Hf_{0.75}Zr_{0.25})B_2$ with minor *m*-(Hf, Zr)O_2
C21-1500-240m	C21		1500	4 h	$(Hf_{0.75}Zr_{0.25})B_2$ with minor *m*-(Hf, Zr)O_2
C22-1500-60m	C22	0.75 : 0.25 : 3 : 20	1500	1 h	$(Hf_{0.75}Zr_{0.25})B_2$ (broad, asymmetric peaks) with minor (Hf, Zr)C
C23-1500-60m	C23	0.75 : 0.25 : 8 : 10	1500	1 h	$(Hf_{0.75}Zr_{0.25})B_2$
C31-700-60m [b]	C31	0.5 : 0.5 : 2 : 10	700	1 h	*t*-$(Hf_{0.5}Zr_{0.5})O_2$ with minor *m*-$(Hf_{0.5}Zr_{0.5})O_2$
C31-800-60m [b]	C31		800	1 h	*t*-$(Hf_{0.5}Zr_{0.5})O_2$ and *m*-$(Hf_{0.5}Zr_{0.5})O_2$
C31P-1500-60m [c]	C31		1500	1 h	$(Hf_{0.5}Zr_{0.5})B_2$ with minor *m*-$(Hf_{0.5}Zr_{0.5})O_2$
C32-1500-60m	C32	0.5 : 0.5 : 2 : 20	1500	1 h	*t*-$(Hf_{0.5}Zr_{0.5})O_2$ with minor (Hf, Zr)C
C33P-1140-60m [c]	C33	0.5 : 0.5 : 3 : 10	1140	1 h	*m*- and *t*- $(Hf_{0.5}Zr_{0.5})O_2$
C33P-1320-60m [c]	C33		1320	1 h	$(Hf_{0.5}Zr_{0.5})B_2$ and *m*-$(Hf_{0.5}Zr_{0.5})O_2$
C33P-1500-5m [c]	C33		1500	5 min	$(Hf_{0.5}Zr_{0.5})B_2$ with minor *m*-$(Hf_{0.5}Zr_{0.5})O_2$
C33P-1500-60m [c]	C33		1500	1 h	$(Hf_{0.5}Zr_{0.5})B_2$
C33-1500-60m	C33		1500	1 h	$(Hf_{0.5}Zr_{0.5})B_2$
C33-1500-60m-E [b]	C33		1500	1 h	$(Hf_{0.5}Zr_{0.5})B_2$ with minor *m*-$(Hf_{0.5}Zr_{0.5})O_2$
C34-1500-60m	C34	0.5 : 0.5 : 3 : 8	1500	1 h	$(Hf_{0.5}Zr_{0.5})B_2$ and *m*-$(Hf_{0.5}Zr_{0.5})O_2$ and minor *t*-$(Hf_{0.5}Zr_{0.5})O_2$
C4-1500-60m	C4	0.25 : 0.75 : 3 : 10	1500	1 h	$(Hf_{0.25}Zr_{0.75})B_2$
C5-1500-60m	C5	0 : 1 : 3 : 10	1500	1 h	ZrB_2

[a] The Hf : Zr : B : C molar ratio is calculated based on the assumption that one mole of sucrose ($C_{12}H_{22}O_{11}$) would yield twelve (12) moles of carbon. Take the example of recipe C33, 1.602 g (0.005 mol) of $HfCl_4$, 1.165 g (0.005 mol) of $ZrCl_4$, 1.855 (0.03 mol) of H_3BO_4, and 2.857 g (0.00835 mol) of sucrose (assumed to yield 0.00835 mol × 12 = 0.100 mol of carbon) would be mixed together, and the starting Hf : Zr : B : C molar ratio = 0.5 : 0.5 : 3 : 10. Such simplification helps empirical optimization of recipes.

[b] These samples were heat treated under "exposed" condition, i.e., the sample was exposed to flowing Ar directly and not placed inside graphite crucible with lid as the other samples.

[c] These samples (C31P- or C33P-) all have a separate pyrolysis step at 800°C for 1 h in flowing Argon after drying of the solution but before the final CTR heat treatment (e.g., at 1500°C). This separate pyrolysis step was initially used to produce the intended oxides-carbon mixture. However, it was not adopted for other samples after finding out the direct heat treatment to the CTR temperature (i.e., without the 800°C pyrolysis step) gave similar results in terms of product phase purity.

in Argon at 700 or 800ºC for 1 h. It showed that the samples after the 700 or 800ºC heat treatment contain (Hf, Zr)O_2 (a mixture of tetragonal *t* and monoclinic *m* phases), while B_2O_3 and carbon presumably exist as amorphous phases.

As the temperature increases further (e.g., closer to ~1500ºC), the endothermic CTR reaction (equation (1)) takes place to produce the metal diboride solid solution. Note in the current study, putting the sample inside the graphite boat with lid helps improve diboride products phase purity: samples with final heat treatment carried out in an open boat (or "exposed") tend to produce significant oxides (see Figure S3B in the supporting document). This is probably because the graphite lid suppresses excessive B_2O_3 evaporation or mitigates oxidation due to impurity in the gas atmosphere. On the other hand, the graphite lid should not be too tight. Otherwise, the graphite boat had been observed to crack after heat treatment, presumably due to pressure build-up caused by release of gases (CO and maybe others) during the heat treatment.

For the BHR method, the same metal precursors of $HfCl_4$ and $ZrCl_4$ were used, while sodium borohydride ($NaBH_4$, 98+%, Acros Organics #13432) was used as the reductant as well as the boron precursor. The recipes are summarized in Table 2. The metal precursors along with $NaBH_4$ powders were hand mixed using a mortar and pestle in an Argon-filled glovebox (VAC Nexus I, Hawthorne, CA, USA) to prevent the precursors from reacting with air or absorbing moisture. (In fact, all starting materials had been stored in the Ar glove box.) The mixed powders were then put into a cylindrical graphite crucible with lid and heat treated in the same way as the CTR method described before. Because in the BHR method the $NaBH_4$ precursor contains Na, the powders after heat treatment were then washed several times with DI water to remove impurities such as sodium chloride (NaCl) and finally rinsed with ethanol and dried on a hotplate set at low temperature (~100°C).

TABLE 2 Summary of starting materials molar ratio, and heat treatment temperature and time, and resulting phase information (from XRD) for $(Hf_{1-x}Zr_x)B_2$ powder samples synthesized via the BHR method. The Hf, Zr, and B sources are $HfCl_4$, $ZrCl_4$, and $NaBH_4$, respectively.

Sample ID	Recipe	Starting Hf : Zr : B molar ratio	Temp (°C)	Holding time	Actual phase(s) from XRD
B3-700-60m	B3	0.5 : 0.5 : 3	700	1 h	$(Hf_{0.5}Zr_{0.5})B_2$ and minor (Hf, Zr)O_2
B3-700-360m	B3		700	6 h	$(Hf_{0.5}Zr_{0.5})B_2$
B3-1500-1m	B3		1500	1 min	$(Hf_{0.5}Zr_{0.5})B_2$ and minor (Hf, Zr)O_2
B3-1500-60m	B3		1500	1 h	$(Hf_{0.5}Zr_{0.5})B_2$

The powers obtained from both synthesis methods were characterized using different techniques. For phase identification, X-ray diffractometer (XRD, Siemens D5000) with Cu-Ka radiation (λ= 1.541874 Å) was used. Powder morphology was characterized by scanning electron microscope (SEM) equipped with energy dispersive X-Ray spectroscopy (EDX) (SEM/EDS, JEOL JSM-6330F) and transmission electron microscopy (TEM, Philips CM-200). Thermogravimetric analysis combined differential scanning calorimetry (TGA-DSC) in air with a constant heating rate of 10 °C/min was carried out for selected powders to determine the thermal oxidation resistance.

2.2 | Flash sintering of $Hf_{0.5}Zr_{0.5}B_2$ powders synthesized by CTR and BHR methods

For flash sintering, $(Hf_{0.5}Zr_{0.5})B_2$ solid solution powders synthesized via both the CTR-based and the BHR methods (powder C33-1500-60m and powder B3-1500-60m) were sintered. The details of the flash sintering setup have been described earlier [20]. Briefly, flash sintering for both types of powders was conducted in a home-made sinter-forging type setup under applied mechanical pressure of ~35 MPa. The synthesized $(Hf_{0.5}Zr_{0.5})B_2$ solid solution powders were hand grinded for ~5 min and loaded inside an insulating hexagonal boron nitride (h-BN) tube (ID of ~3.1 mm), and graphite top and bottom electrodes were used to provide electrical contact. This way, upon the application of a constant DC electrical voltage

of 8 V (electrical field of ~32 V/cm), all current is forced to only pass through the powder compact. Note that when using the CTR powder, even without external preheating of the sample assembly, the measured current increased first slowly and then rapidly until reaching a preset limit of 190 A (or 25.2 A/mm^2) for sintering. When using the BHR powder, the sample assembly had to be externally heated to ~500°C before the current started to increase rapidly to a preset limit of 200 A (or 26.5 A/mm^2). After reaching the limiting current, the power supply was programmed to switch to the constant current mode and maintained at the limiting current (190 A for the CTR powder or 200 A for the BHR powder) for another 120 s. The current and voltage data were recorded by the LabView software.

It should be mentioned that the current home-made flash sintering setup does have limitations in at least two aspects. First, although a thermocouple was incorporated in the system, its tip was placed at a distance several millimeter away from the sample surface. Therefore, although a *nominal* temperature is recorded, the value is *much lower* than the actual sample temperature during the flash sintering experiment, and the difference could be hundreds of degree Celsius or even larger, as shown in our earlier study [20]. Second, the current flash sintering experiments were all carried out in *air*. However, because the small diboride samples were sandwiched between the top and bottom graphite electrodes and enclosed within h-BN tubes, and all those parts (sample, graphite electrodes, h-BN tubes) were then enclosed within a large graphite tube, the diboride samples were protected from thermal oxidation during the flash sintering experiment, despite the observation that the set-up assembly heated up considerably and became red hot (see our earlier study [20] for more details). The authors are in the process of improving the system to address these issues for future studies.

Nevertheless, after flash sintering, the samples had diameter of ~3.1 mm and thickness typically shrank from ~2.5 mm to ~2 mm. The microstructure and local composition of the flash sintered ceramic samples were characterized by SEM and EDS (typically acceleration voltage of 25-30 kV, at magnification of 1000 to 5000). The relative density was estimated from sample weight and dimension (Archimedes method was not used due to very small sample size). The Vickers hardness test was performed with a LECO LM810AT hardness tester. The load applied was 1000 gm of force (gf), and the dwell time was 10 sec. The hardness was recorded 10 times at different surface locations for each sample. TGA-DSC in air was also obtained for small pieces from the flash sintered samples to evaluate the thermal oxidation resistance of the bulk $(Hf_{0.5}Zr_{0.5})B_2$ solid solution.

3 | RESULTS AND DISCUSSION

3.1 | $(Hf_{1-x}Zr_x)B_2$ single-phase solid solution powders synthesized via CTR based method

Table 1 summarizes the $(Hf_{1-x}Zr_x)B_2$ solid solution powder samples with different nominal compositions synthesized via the CTR-based method. The recipe number, starting Hf : Zr : B : C molar ratio, the final CTR heat treatment temperature and time, and the resulting phase information from XRD are provided.

3.1.1 | $(Hf_{0.5}Zr_{0.5})B_2$

Figure 1 shows the XRD patterns for selected samples targeting $(Hf_{0.5}Zr_{0.5})B_2$ solid solution with final CTR heat treatment at different temperature from 1140 to 1500°C. The starting Hf : Zr : B : C molar ratio was 0.5 : 0.5 : 3 : 10 (from recipe C33), meaning boron was 50% excess by molar, while carbon has 100% excess comparing with the idealized CTR reaction (see equation (1) before). Note that for the 1500°C-1 h sample, XRD showed a single set of diffraction peaks matching hexagonal MgB_2-type structure without any hint of peak splitting or phase separation. The calculated lattice constants were a =3.156 Å and c = 3.502 Å, which are in good agreement with the values of a = 3.155 Å and c = 3.497 Å for $(Hf_{0.5}Zr_{0.5})B_2$ single-phase solid solution (JCPDS# 01-0745-449), which suggest the synthesis of the single phase solid solution powder was successful under this condition. On the other hand, when the CTR temperature was as low as 1140°C, there were no diboride phase: only crystalline (Hf, Zr)O_2 (partly monoclinic and partly tetragonal) could be identified in the products, while both boron oxide and carbon remained as amorphous phases. When the CTR temperature was intermediate at 1320°C, the CTR reaction started to occur, but was not complete. Apart from the single phase $(Hf_{0.5}Zr_{0.5})B_2$ solid solution, the XRD pattern revealed significant amount of (Hf, Zr)O_2, primarily as the monoclinic phase with a small amount of tetragonal phase.

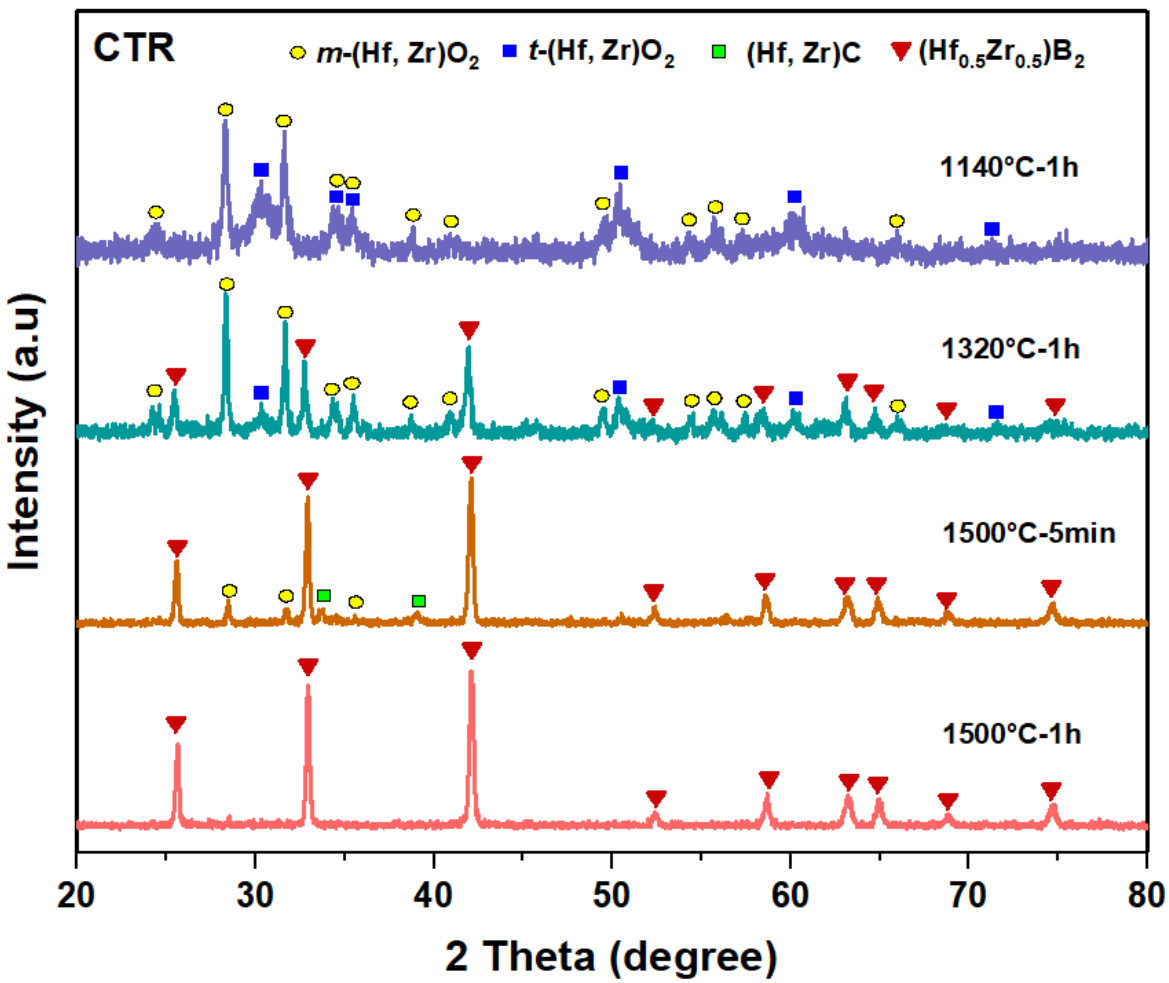

FIGURE 1 XRD patterns for powder samples targeting $(Hf_{0.5}Zr_{0.5})B_2$ synthesized via the CTR-based method with final heat treatment in Ar at different temperatures for different time. All four samples (C33P-1140-60m, C33P-1320-60m, C33P-1500-5m, C33P-1500-60m) are from the same recipe of C33 with starting Hf : Zr : B : C molar ratio = 0.5 : 0.5 : 3 : 10, meaning boron has 50% excess, while carbon has 100% excess.

Figure 1 also includes the XRD pattern for a $(Hf_{0.5}Zr_{0.5})B_2$ powder synthesized via CTR at 1500°C but with shorter time of 5 min. It shows that the CTR reaction kinetics was quite fast at 1500°C. Even after only 5 min, the $(Hf_{0.5}Zr_{0.5})B_2$ solid solution formation was largely complete with only minor residual (Hf, Zr)O_2 (and, presumably, some unreacted amorphous B_2O_3 and carbon). Comparison of XRD for the 1500°C samples (e.g., 5 min and 1 h) with those at lower temperature (e.g., 1320°C-1 h, 1140°C-1 h) suggests that both higher CTR temperature and longer reaction time promotes the diboride solid solution formation from the oxides, yet temperature seems to play the more dominant role. This is expected when considering thermodynamics for the system.

The standard Gibbs free energy change (ΔG^o) for CTR reactions to form both HfB_2 and ZrB_2 from the individual oxides (see below)

$$HfO_2 + B_2O_3 + 5C = HfB_2 + 5CO \quad (3)$$

$$ZrO_2 + B_2O_3 + 5C = ZrB_2 + 5CO \quad (4)$$

are calculated using the thermochemical data of pure substances [21] and plotted as a function of CTR temperature as shown in Figure S4. Under standard pressure (P_{CO} = 1 atm), ΔG^o for the formation of HfB_2 and ZrB_2 are similar and turns negative when temperature exceeds ~1500°C, meaning the formation of

those diborides from CTR reactions becomes energetically favorable at temperatures of ~1500°C or higher. Of course, Argon gas flow might lead to some drop in P_{CO} and shift the critical temperature to lower, which is consistent with the observation of some diboride solid solution formation at lower temperature such as 1320°C.

As to the impact of starting recipe or molar ratio between metal, boron, and carbon precursors, note that because B_2O_3 evaporates at elevated temperature, it seems necessary to have some boron excess [1, 22]. Figure 2A is the XRD pattern for a sample synthesized via the CTR-based method at 1500°C for 1h from recipe C33 with 50% excess boron and the same 100% carbon excess, targeting total metal (i.e., Hf + Zr) or M : B : C molar ratio = 1 : 3 : 10. As before, the XRD showed only $(Hf_{0.5}Zr_{0.5})B_2$ solid solution. For comparison, Figure 2B shows XRD pattern for a sample from recipe C31 with no excess boron and the same 100% carbon excess, i.e., targeting M : B : C molar ratio = 1 : 2 : 10. The sample contained significant residual monoclinic (Hf, Zr)O_2 apart from $(Hf_{0.5}Zr_{0.5})B_2$. In addition, Figure 2C shows XRD pattern for a sample from recipe C34 with the same 50% boron excess but *reduced excess carbon* (only 60% excess) targeting M : B : C molar ratio = 1 : 3 : 8. The sample contained significant amount of (Hf, Zr)O_2, indicating that some carbon excess was also necessary to ensure high product purity in the current CTR-based method. This is because the actual carbon yield for sucrose during the heat treatment was lower than the theoretical value (~42.1% by weight).

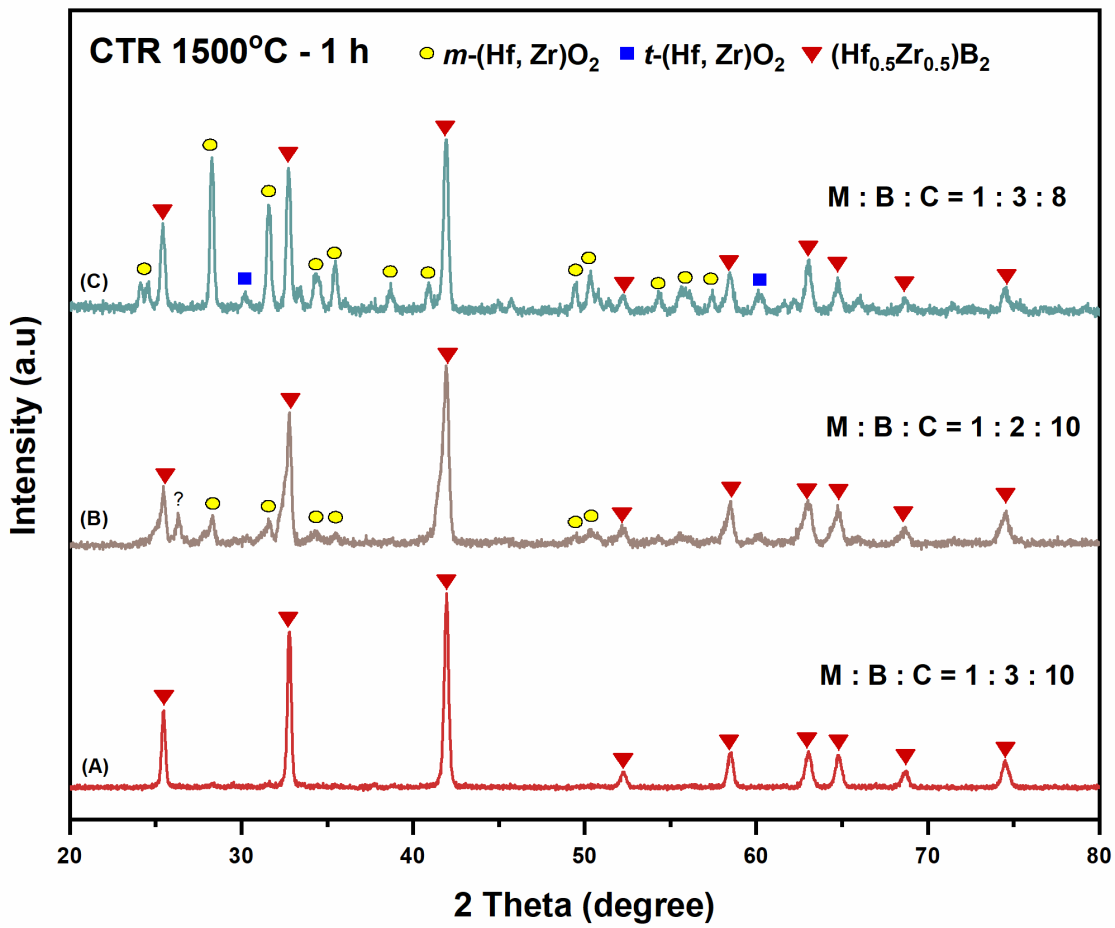

FIGURE 2 XRD patterns for powder samples targeting $(Hf_{0.5}Zr_{0.5})B_2$ synthesized via the CTR-based method with final 1500°C-1 h heat treatment using different recipes: (A) C33 of starting total metal M : B : C molar ratio = 1 : 3 : 10 (sample C33P-1500-60m), (B) C31 of starting total metal M : B : C molar ratio = 1 : 2 : 10 (sample C31P-1500-60m), (C) C34 of starting M : B : C molar ratio = 1 : 3 : 8 (sample C34-1500-60m). ? represents unidentified phase from XRD.

3.1.2 | Other compositions for $(Hf_{1-x}Zr_x)B_2$ and complications

$(Hf_{1-x}Zr_x)B_2$ single-phase solid solution powders with Hf : Zr ratio different from 0.5 : 0.5 were also synthesized using the CTR-based method. Figure 3A shows XRD patterns for $(Hf_{1-x}Zr_x)B_2$ powders with x = 0, 0.25, 0.5, 0.75, and 1, all synthesized at 1500°C for 1 h in Ar from recipes with the same total M : B : C molar ratio of 1 : 3 : 10, i.e., 50% boron excess and 100% carbon excess (see Table 1 for details). All compositions displayed a single set of narrow diffraction peaks matching the hexagonal MgB_2 structure, suggesting diboride solid solution formation. In particular, Figure 3B is the zoomed-in section of the (101) diffraction peak, which clearly shows gradual shift to lower angle for the solid solution with increasing x or Zr content (or decreasing Hf content). The observation is consistent with Vegard's law in that the lattice parameter expands when the smaller Hf atoms are replaced by the larger Zr atoms in the $(Hf_{1-x}Zr_x)B_2$ solid solution. In addition, Figure 3B shows that the (101) peaks for all samples are largely symmetric, indicating absence of obvious phase separation.

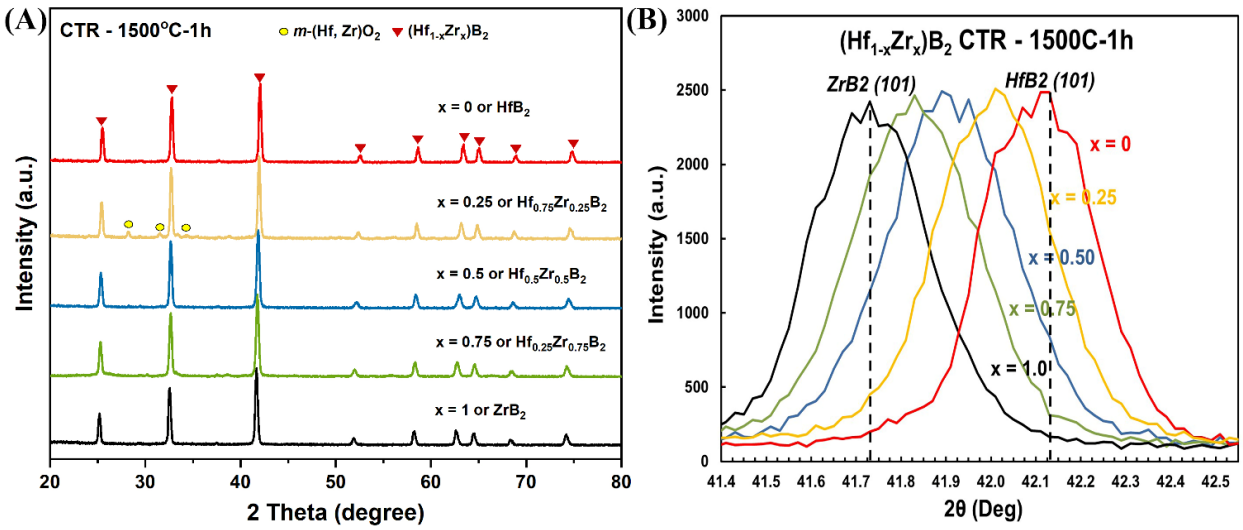

FIGURE 3 A, XRD patterns for $(Hf_{1-x}Zr_x)B_2$ solid solution powders synthesized via the CTR-based method with final heat treatment at 1500°C for 1h in Ar targeting five different compositions (x = 0, 0.25, 0.5, 0.75, and 1); B, Zoom-in section of the (101) diffraction peaks showing the gradual shift of diffraction peaks to lower angle for five $(Hf_{1-x}Zr_x)B_2$ solid solution powders, indicating continuous expansion of lattice parameters with increasing x or Zr content.

However, it is noted from Figure 3A that among the different $(Hf_{1-x}Zr_x)B_2$ solid solution powders synthesized using the CTR-based method at 1500°C for 1 hour, the one targeting x = 0.25 or $(Hf_{0.75}Zr_{0.25})B_2$ (sample C21-1500-60m) contained some residual (Hf, Zr)O_2, apart from the major diboride phase. This is surprising given that (i) all five powders are based on the same starting total M : B : C molar ratio of 1 : 3 : 10, and (ii) Figures 3A shows that both end compositions of x = 0 and x = 1 form pure phases (HfB_2 and ZrB_2, respectively) without identifiable residual oxides, and (iii) repeated experiments yielded similar results.

To understand the origin for the persistence of some residual (Hf, Zr)O_2 for the $(Hf_{0.75}Zr_{0.25})B_2$ sample, a few additional experiments were carried out. The first involves carrying out CTR-based synthesis using the same C21 recipe but with *longer holding time* of 4 h at 1500°C instead of 1 h. The purpose is to see if the residual (Hf, Zr)O_2 is due to inadequate CTR reaction time. However, after 4 h, the product still contained (Hf, Zr)O_2 - in fact, the relative peak intensity for the residual (Hf, Zr)O_2 became stronger, as shown in Figure 4A for sample C21-1500-240m, which suggests the residual oxide is not due to slow kinetics or inadequate CTR reaction time. Instead, it might be related to *depletion* of one (or more) of the reactants. The second experiment shows that when the sucrose (as carbon precursor) content was doubled

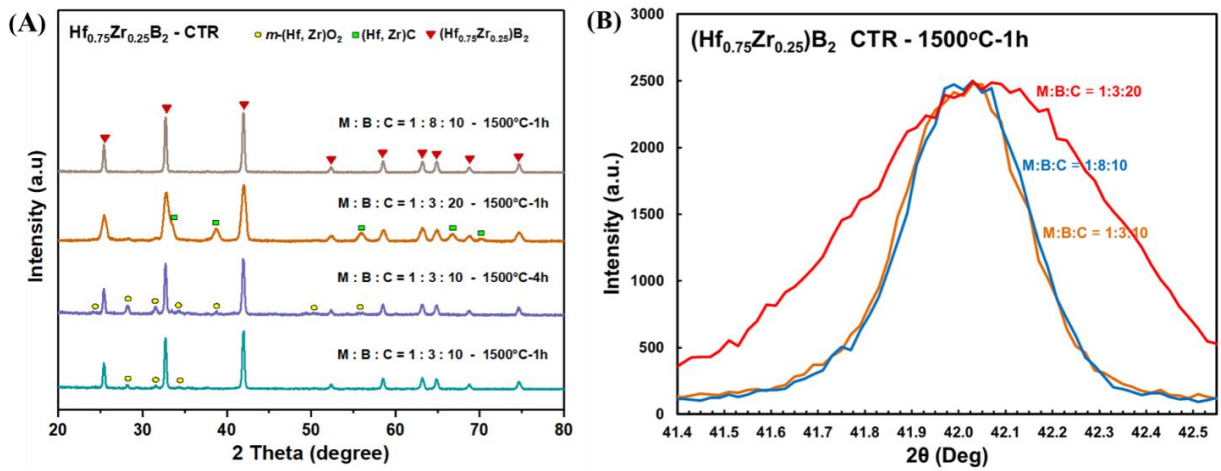

FIGURE 4 A, XRD patterns for $(Hf_{0.75}Zr_{0.25})B_2$ powder samples synthesized via the CTR-based method at 1500°C from different recipes: sample ID from the bottom to the top are C21-1500-60m (starting total M : B : C molar ratio = 1 : 3 : 10), C21-1500-240m (M : B : C = 1 : 3 : 10), C22-1500-60m (M : B : C = 1 : 3 : 20), and C23-1500-60m (M : B : C = 1 : 8 : 10). See Table 1 for more details. B, Zoom-in section of the (101) diffraction peaks for three of the samples, all heat treated at 1500°C for 1 h, showing significant peak broadening and asymmetry for the sample with too much carbon, i.e., from recipe C22 with starting M : C molar ratio = 1 : 20 or 300% carbon excess.

so that starting total metal to carbon or M : B molar ratio was 1 : 20 (300% excess) while boron content was kept the same at 50% excess, although (Hf, Zr)O_2 were largely removed, significant carbide solid solution or (Hf, Zr)C remained, as shown in Figure 4A for sample C22-1500-60m. The third experiment showed that, when boron (essentially H_3BO_3) content was increased in the recipe so that the starting total M : B molar ratio was 1 : 8, i.e., 300% boron excess comparing with the typical 1 : 3 or 50% boron excess for samples in Figure 3, while the carbon precursor (sucrose) was kept the same (starting M : C molar ratio of 1 : 10 or 100% excess), the powder product contained no remaining (Hf, Zr)O_2, as shown in Figure 4A for sample C23-1500-60m. The complete elimination of residual oxides upon addition not of more carbon precursor (sucrose) but of more H_3BO_3 suggests that the complete CTR reaction for the system targeting Hf : Zr = 3 : 1 and 50% boron excess at 1500°C is limited by boron (depletion) and not carbon.

From a first look, such a complication is unexpected because the same 50% boron excess and the same 100% carbon excess deliver $(Hf_{1-x}Zr_x)B_2$ solid solution phases without (Hf, Zr)O_2 for all the other four compositions studied, i.e., x = 0, 0.5, 0.75, and 1. One hypothesis is that this phenomenon is related to the monoclinic to tetragonal ($m \rightarrow t$) phase transformation in the HfO_2-ZrO_2 system. Specifically, according to the monotonic HfO_2 - ZrO_2 phase diagram, HfO_2 and ZrO_2 form a complete solid solution, and there is a phase transformation from the low temperature stable monoclinic phase to the intermediate temperature stable tetragonal phase. The equilibrium temperature for the $m \rightarrow t$ phase transformation of (Hf, Zr)O_2 depends on the Hf : Zr ratio: it decreases continuously from ~1750°C for pure HfO_2 (x = 0) to ~1100°C for pure ZrO_2 (x = 1) [23]. As a first approximation using linear interpolation, the equilibrium $m \rightarrow t$ phase transformation temperature is estimated to be ~1588°C for x = 0.25 or $(Hf_{0.75}Z_{r0.25})O_2$, ~1425°C for x = 0.5 or $(Hf_{0.5}Z_{r0.5})O_2$, and ~1263°C for x = 0.75 or $(Hf_{0.25}Z_{r0.75})O_2$.

The implication from such analysis is that for the other three compositions of x = 0, 0.75, and 1, the $m \rightarrow t$ phase transformation for (Hf, Zr)O_2 would *not* interfere with the CTR reaction to form the diborides. In particular, for x = 0 (Hf : Zr = 1 : 0), the $m \rightarrow t$ phase transformation of HfO_2 would not come into play since the equilibrium transformation temperature of 1750°C is much higher than the actual heat treatment temperature of 1500°C. On the other hand, for x = 0.75 (Hf : Zr = 0.25 : 0.75) and x = 1 (Hf : Zr = 0 : 1), the (Hf, Zr)O_2 $m \rightarrow t$ phase transformation has already finished (at ~1263 or ~1100°C, respectively) before the furnace reaches 1500°C for the CTR reaction. In fact, even for the composition of x = 0.5 (Hf : Zr = 1

: 1), the equilibrium $m \rightarrow t$ phase transformation temperature is ~1425ºC. The consequence will be that when the furnace is heated up to 1500ºC for CTR, the (Hf, Zr)O_2 $m \rightarrow t$ phase transformation has also already finished.

In comparison, for x = 0.25 (Hf : Zr = 0.75 : 0.25), the estimated equilibrium temperature is 1588ºC. The Zr impurity in $HfCl_4$ means the real equilibrium temperature for the (Hf, Zr)O_2 $m \rightarrow t$ phase transformation in this sample might be lower than 1588ºC and close to the CTR temperature of 1500ºC. Considering that the (Hf, Zr)O_2 $m \rightarrow t$ phase transformation is endothermic, it might compete with the endothermic CTR reaction (equation (1)) for heat input and slow down the CTR reaction. Meanwhile, B_2O_3 (from H_3BO_3) is known to evaporate rapidly at above ~1000ºC [22] and starts to sublime at ~1500ºC [24]. Any delay in the CTR reaction due to heat absorption from the $m \rightarrow t$ phase transformation for (Hf, Zr)O_2, as mentioned, means more B_2O_3 (than the 50% excess included for recipe C21) might escape from the system while not leaving enough for the completion of the CTR reaction. As a result, some (Hf, Zr)O_2 remains as one of the residual phase(s), as shown in Figures 3A and 4A [22].

One last point worth mentioning is that although excess carbon is also needed to ensure complete CTR reaction and removal of oxides (see earlier discussion and Figure 2), too much carbon (from sucrose addition) also inhibits the formation of uniform solid solution. To illustrate this, Figure 4B shows the zoomed section of the (101) diffraction peaks for three samples with the same Hf : Zr ratio of 0.75 : 0.25 and same final CTR heat treatment at 1500ºC for 1 h. The diffraction peak for sample C22-1500-60m with initial M : C molar ratio = 1 : 20 (nominally 300% carbon excess) is significant broader and more asymmetric comparing to the other two samples-both with total M : C = 1 : 10 (nominally 100% carbon excess), despite the variation in boron content for the later two. Such an observation is explained by the effect of excess carbon on limiting cation (Hf and Zr) inter-diffusion. Specifically, it has been reported that carbon vacancies enhance cation diffusion for high temperature ceramics [25], while excess carbon is expected to suppress formation of carbon vacancies. Excess of carbon, as secondary phase, also creates additional interfaces between the diboride phases formed in CTR. Both these effects are expected to slow down the cation interdiffusion (between Hf and Zr) and the formation of a uniform diboride solid solution, giving rise to the broadening and asymmetry of the XRD peaks, as seen in Figure 4B.

3.2 | $(Hf_{0.5}Zr0._5)B_2$ single-phase solid solution powder synthesized via BHR method

Apart from CTR-based method described above, $(Hf_{1-x}Zr_x)B_2$ solid solution powders were also synthesized via the BHR method in which Hf and Zr chlorides are reacted directly with $NaBH_4$. Figure 5 shows the XRD patterns for $(Hf_{0.5}Zr_{0.5})B_2$ solid solution powders from the BHR method using recipe B3. With 1500ºC-1 h heat treatment and subsequent water washing, the powder gave a single set of diffraction peaks matching $(Hf_{0.5}Zr_{0.5})B_2$ single-phase solid solution with no crystalline oxides or other impurities. The calculated lattice constants of a = 3.153 Å and c = 3.500 Å were in good agreement with a = 3.155 Å and c = 3.497 Å for JCPDS# 01-0745-449. When the heat treatment temperature was reduced to 700°C, the XRD patterns still showed $(Hf_{0.5}Zr_{0.5})B_2$ single-phase solid solution and the diffraction peaks were very broad, indicating very small crystallite[14]. This indicates that the formation of (Hf, Zr)B_2 via the BHR process does not appear to be thermodynamically limited. It occurred over a wide temperature window down to 700ºC. This is in contrast to the CTR-based synthesis method for which there is almost no reaction between oxides and carbon at ~1140ºC and below, as shown in Figure 1.

Note that Figure 5 also shows that B3-700-60m and B3-1500-1m samples are largely pure with some minor oxide impurities, which are removed by longer heat treatment at the respective temperature. The appearance of minor oxides is attributed to impurities, especially oxides or hydroxides in the starting

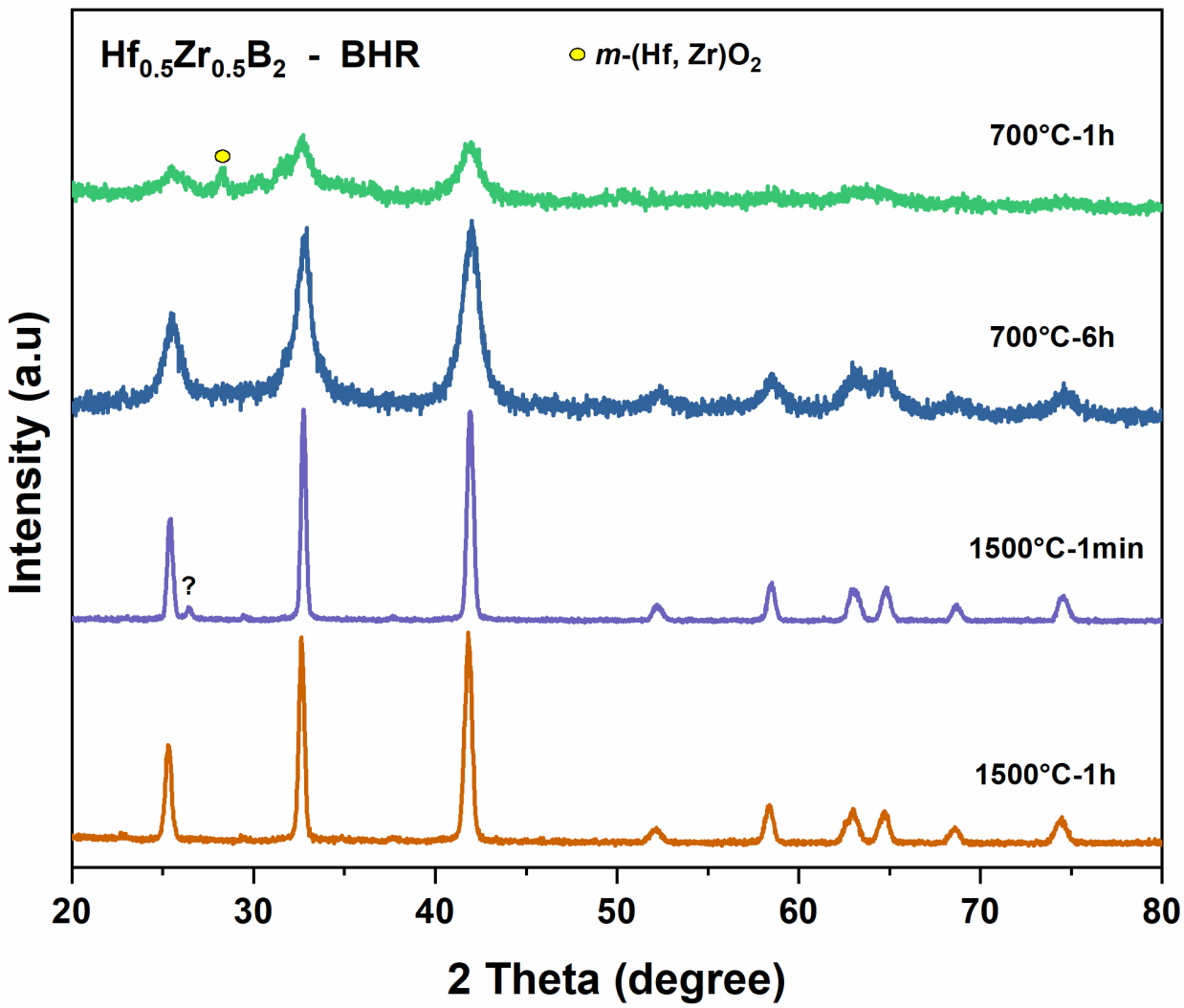

FIGURE 5 XRD patterns of $(Hf_{0.5}Zr_{0.5})B_2$ solid solution powders synthesized via the BHR method from recipe B3 (starting Hf : Zr : B molar ratio = 0.5 : 0.5 : 3) at 700°C or 1500°C for different time. The sample IDs from the bottom to the top are: B3-1500-60m, B3-1500-1m, B3-700-360m, and B3-700-60m, respectively.

material, as a result of reactants ($HfCl_4$, $ZrCl_4$, and $NaBH_4$) in contact with air/moisture during storage and handling. The observation here is consistent with previous reports on diboride formation from reaction between HfO_2 or ZrO_2 with $NaBH_4$ at temperature as low as 700ºC [26].

3.3 | Characterization of $(Hf_{0.5}Zr_{0.5})B_2$ powders synthesized via CTR and BHR methods

3.3.1 | SEM and TEM

Microstructures for selected powder samples were characterized using SEM and TEM. In particular, Figure 6A shows SEM images for the $(Hf_{0.5}Zr_{0.5})B_2$ powder synthesized via the CTR-based method with final heat treatment at 1500ºC for 1 hour. Most of the grains were submicrometer but highly agglomerated. However, the powder displays some non-uniformity with variation in grain size from near-micron-sized faceted particles to much finer nanocrystals. SEM for $(Hf_{0.5}Zr_{0.5})B_2$ powders synthesized via the BHR method at 1500°C for 1 hour is shown in Figure 6B. The morphology also displays some non-uniformity, but the grains mostly below the micron.

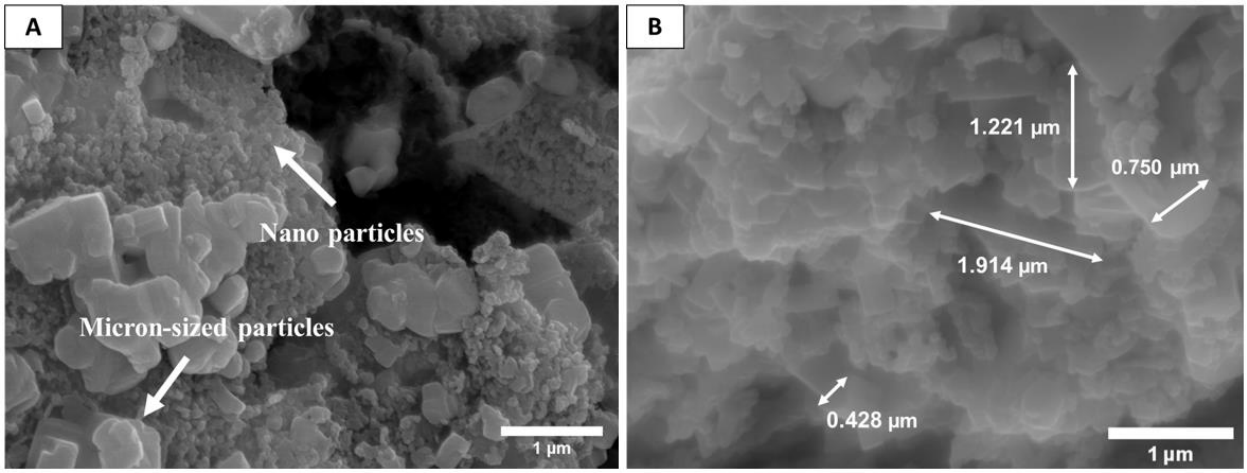

FIGURE 6 SEM micrographs of $(Hf_{0.5}Zr_{0.5})B_2$ solid solution powders synthesized at 1500ºC for 1 h via both the CTR-based method (A) and the BHR method (B): A is for sample C33-1500-60m with starting Hf : Zr : B : C molar ratio of 0.5 : 0.5 : 3 : 10; B is for sample B3-1500-60m with starting Hf : Zr : B = 0.5 : 0.5 : 3.

TEM images and a corresponding selected area electron diffraction (SAED) pattern for the $(Hf_{0.5}Zr_{0.5})B_2$ solid solution powders synthesized via the CTR-based method (sample C33-1500-60m) and the BHR-based method (sample B3-700-360m) are shown in Figure 7. The particles from the CTR-based method were covered by an amorphous carbon layer of ~3-4 nm thick. The powders from the BHR method were also covered by an amorphous layer. However, the amorphous layer is *unlikely* to be carbon since the reactants in BHR method did not contain carbon. Most likely it consisted of low boiling point amorphous phase of Na and B that could be evaporated by further heat treatment. In fact, when the powder sample B3-700-360m was further annealed at 1500 C for 3 hours, it lost 37.1% of its weight and developed much larger grains as shown in Figure S5 (A). The SAED pattern shows diffraction rings from the inner to the outer region and were attributed to the (001), (100), (101) and (201) planes for $(Hf_{0.5}Zr_{0.5})B_2$ from the CTR method. The measured d-spacing from the high resolution TEM (HRTEM) lattice fringes was ~3.5 Å, as shown in Figure 7B, which is close to the expected value of 3.497 Å for the (001) plane of the hexagonal $(Hf_{0.5}Zr_{0.5})B_2$ (JCPDS# 01-0745-449).

3.3.2 | Oxidation resistance of $(Hf_{0.5}Zr_{0.5})B_2$ powders

The thermal oxidation resistance of $(Hf_{0.5}Zr_{0.5})B_2$ solid solution powders synthesized via both the CTR-based method and the BHR method at 1500°C for 1 hour was evaluated by TGA-DSC in air, and the results are shown in Figure 8. For the CTR powder (C33-1500-60m), as shown in Figure 8A, during the initial heating up to ~600ºC, there was no obvious change in sample weight nor heat-related phenomena. Stating from ~650ºC, there was a significant weight gain up to 38.9% at ~1000°C, and the corresponding exothermic peak was at ~720°C. The weight gain can be attributed to the oxidation of $(Hf_{0.5}Zr_{0.5})B_2$ solid solution powder to form (Hf, Zr)O_2 solid solution as well as B_2O_3 (l) [13, 14]. It is interesting to note the DSC curve showed wo partially overlapping exothermic peaks: one sharper at ~720ºC and the other broader at ~770ºC. When compared to the theoretical weight gain of 51% for stoichiometric $(Hf_{0.5}Zr_{0.5})B_2$ complete oxidation without B_2O_3 evaporation, the observed maximum weight gain of 38.9% at 1000ºC was lower. The lower weight gain than theoretical during oxidation might be attributed to related to B_2O_3 evaporation [22]. In fact, TGA showed that beyond ~1000°C, the sample began to lose weight, and the weight loss greatly accelerated at ~1200ºC. Another possibility is related to weight loss due to oxidation of residual carbon in the powder. The final weight gain was 26.1% at 1490°C, which is much lower than the 51% value for complete oxidation without B_2O_3 evaporation but still much higher than the 6.6% value expected

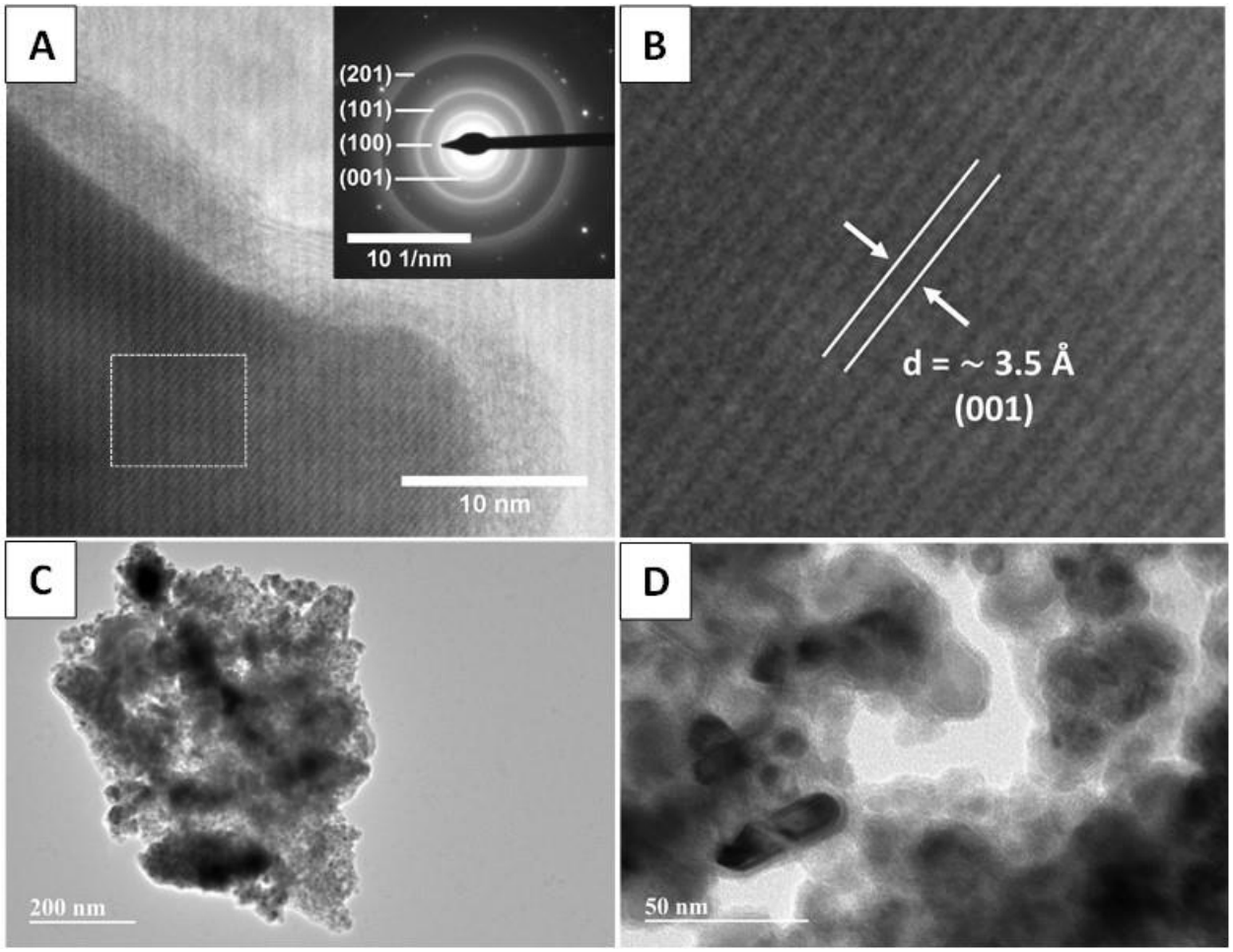

FIGURE 7 TEM (A, C and D) and HR-TEM (B) micrographs of $(Hf_{0.5}Zr_{0.5})B_2$ solid solution powders of (A, B) C33-1500-60m synthesized via the CTR-based method at 1500°C for 1 hour and (C, D) B3-700-360m synthesized via the BHR-based method at 700°C for 6 hours. A corresponding SAED pattern is also included in A, which shows diffraction rings from the inner to the outer attributed to (001), (100), (101) and (201) crystal planes of the diboride solid solution. The measured d-spacing from the TEM lattice fringes is ~3.5 Å, which is close to the expected value of 3.497 Å for the (001) plane of $(Hf_{0.5}Zr_{0.5})B_2$. Note the surface of the CTR powder is covered by amorphous carbon (A), while the surface of the 700°C-6 h BHR powder is also covered by significant amount of amorphous material (D).

for complete $(Hf_{0.5}Zr_{0.5})B_2$ oxidation with all B_2O_3 evaporated, indicating some B_2O_3 must have remained after the TGA oxidation.

Figure 8B shows the result for the BHR powder (B3-1500-60m). During the initial heating from room temperature to ~400°C, there was a small weight loss of 0.27%, which might be attributed to moisture removal. From 400 to 700°C there was a gradual weight gain of 2.3%. At ~700°C, the weight gain accelerated with an instantaneous jump to ~10% and then slowed down somewhat. The recorded maximum weight gain was ~47% at ~1100°C. Similar to the CTR powder, there were also two exothermic peaks in the DSC curve, which corresponds well with the TGA curve and also hints a two-stage oxidation process. The first stage had a sharp exothermic peak at ~717°C, and the corresponding weight gain is ~10%. It is tentatively attributed to the oxidation of $(Hf_{0.5}Zr_{0.5})B_2$ solid solution to $(Hf_{0.5}Zr_{0.5})B_2O$ (theoretical weight

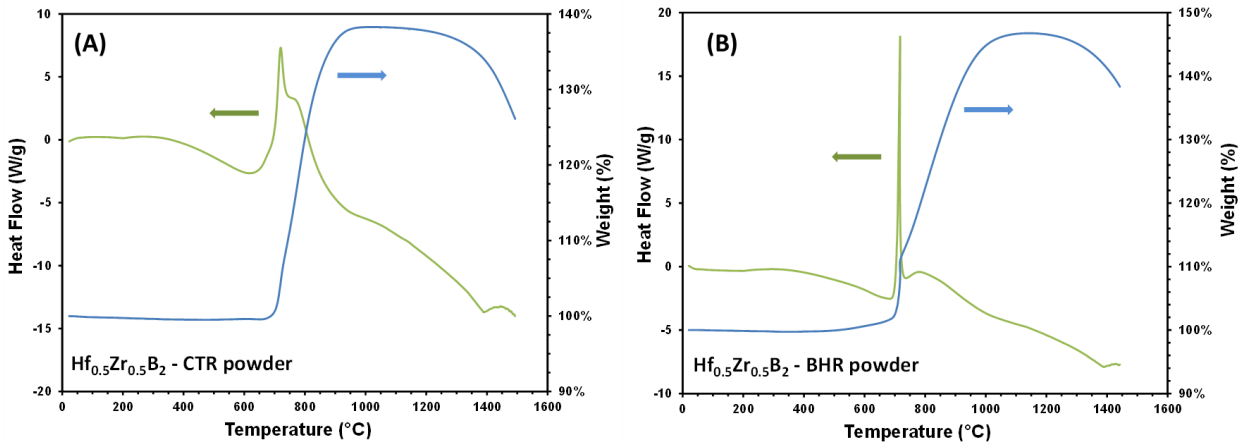

FIGURE 8 TGA and DSC curves in air for $(Hf_{0.5}Zr_{0.5})B_2$ solid solution powders synthesized at 1500°C for 1 hour in Argon via (A) the CTR-based method or (B) the BHR method. The heating rate was 10°C/min. Note for the CTR powder (C33-1500-60m), the starting Hf : Zr : B : C molar ratio = 0.5 : 0.5 : 3 : 10; for the BHR powder (B3-1500-60m), the starting Hf : Zr : B molar ratio = 0.5 : 0.5 : 3.

gain of 10.2%). The second stage had a lower and broader exothermic peak centered at ~750°C, and the continued oxidation leads to formation of (Hf, Zr)O_2 solid solution and B_2O_3 [13, 14], just like the CTR powder. The observed total weight gain of 47% at ~1100°C is still lower but much closer to the expected value of 51% for $(Hf_{0.5}Zr_{0.5})B_2$ complete oxidation without B_2O_3 evaporation, suggesting the 1500°C BHR powder had higher purity than the CTR powder, most likely because the BHR powder had much less residual (amorphous) carbon. Upon further increase in temperature to ~1200°C, mass loss due to B_2O_3 vaporization became obvious and it accelerated greatly at above ~1300°C and the final weight gain was ~38% at 1490°C.

3.4 | Flash sintering of $(Hf_{0.5}Zr_{0.5})B_2$ powders

Figure S6 shows change of current and nominal temperature versus time when 8 V DC was applied for flash sintering of $(Hf_{0.5}Zr_{0.5})B_2$ solid solution powders from both the CTR-based method (C33-1500-60m) and the BHR method (B3-1500-60m) [20]. The entire sintering process was very short: less than ~200 sec for the CTR powder and less than 300 sec (including pre-heating) for the BHR powder. As mentioned, the resistance of the green pellet (3.1 mm diameter and ~2.5 mm initial thickness) from the CTR powder was low enough for the flash event (i.e., the rapid increase in electrical current as well as temperature) to occur at room temperature without preheating. In comparison, for the BHR powder, the sample assembly (see our earlier study [20]) had to be pre-heated to ~500°C for the flash to occur. This difference might be attributed to the presence of excess carbon in the CTR powder (see TEM image in Figure 7 and the discussion about TGA oxidation of both powders in Figure 8) or the less conductive amorphous phase covering the BHR sample. The measured relative density (based on dimension and weight) after flash sintering was ~70% and ~95% for the samples from the CTR and BHR powder, respectively.

Note that Figure S6 shows the highest nominal temperature recorded during the flash sintering was only up to ~1400°C for the CTR powder and ~1150°C for the BHR powder. These temperatures, especially for the BHR powder, appear too low to realize the high relative density for the highly refractory Hf-Zr diboride solid solution. As explained in the experimental section, the low temperature measured is a major limitation of the current in-house system. The thermocouple was at several millimeters away from the sample surface and its position was not controlled with high precision, which led to large difference between the measured nominal temperature and sample actual temperature. (Placing the thermocouple tip too close did not help because the center temperature was enough to melt the thermocouple tip. On the other hand, optical

measurement based on thermal radiation is not yet available for the current set-up.) In fact, the very large difference between reported nominal temperature and actual sample temperature has been reported for FSPS of ultrahigh temperature ceramics. For example, Zou et al. carried out FSPS of HfB_2 and observed that the nominal temperature measured was only up to ~1250°C in the graphite electrode, while the HfB_2 sample was sintered to >95% relative density within only ~20 sec, indicating real sample temperature of ~2200°C or even higher [16, 17].

Figure 9 shows SEM images of fractured surface for bulk $(Hf_{0.5}Zr_{0.5})B_2$ solid solution after flash sintering from both CTR and BHR powders. As shown in Figure 9A, the sample from the CTR powder was porous and contained two phases: the faceted crystalline phase corresponds to the $(Hf_{0.5}Zr_{0.5})B_2$ solid solution, while the other flaky and layered phase most likely corresponds to residual carbon in the CTR powder. The grain size for $(Hf_{0.5}Zr_{0.5})B_2$ in this sample was about 3 μm. In comparison, Figure 9B shows that the flash sintered sample from the BHR $(Hf_{0.5}Zr_{0.5})B_2$ powder was much denser with closed pores. The grain size was about 10 μm. EDS analysis indicates Hf to Zr atom ratio of around 1.01 ± 0.15 for the flash sintered sample from CTR powder and 1.26 ± 0.31 for the flash sintered sample from the BHR powder. The higher Hf : Zr ratio than the expected 1 : 1 ratio for the sample from BHR powder indicates some Zr loss in the BHR synthesis process, and the reason is still under investigation. Note that due to instrument limitation, the B to total metal (Hf + Zr) ratio was not reliable for our EDS and not reported here.

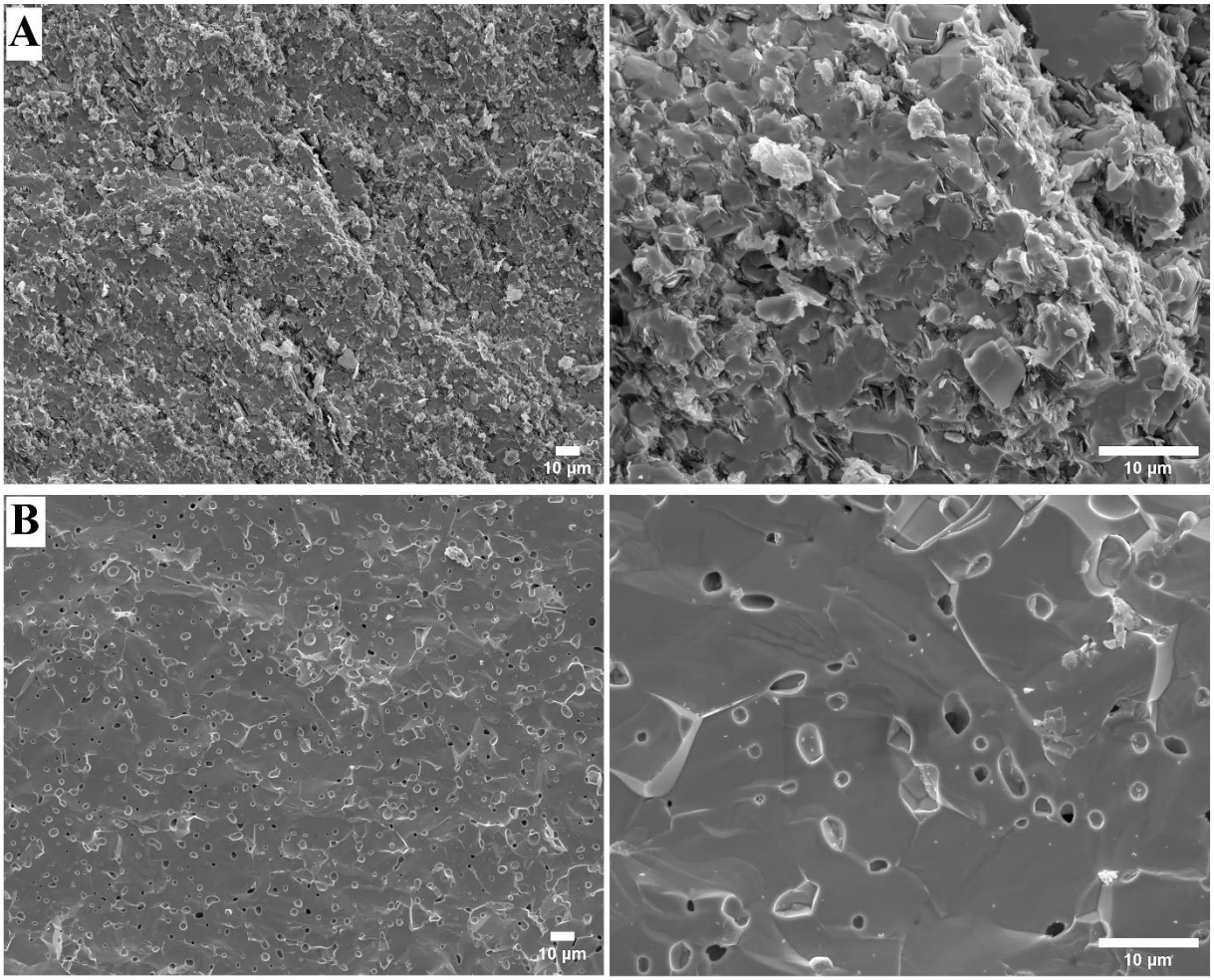

FIGURE 9 SEM images of fractured surface for bulk $(Hf_{0.5}Zr_{0.5})B_2$ solid solution flash sintered from (A) the CTR powder C33-1500-60m and (B) the BHR powder B3-1500-60m.

3.5 | Properties of flash sintered $(Hf_{0.5}Zr_{0.5})B_2$ solid solutions

The measured Vickers hardness for the flash sintered bulk $(Hf_{0.5}Zr_{0.5})B_2$ ceramics from the CTR powder (C33-1500-60m) was 8.23 ± 0.10 GPa, which is significantly lower than the reported values of 21-22 and 27-28 GPa [27] for bulk HfB_2 and ZrB_2, respectively. In comparison, the measured Vickers hardness was 23.01 ± 0.37 GPa for the flash sintered $(Hf_{0.5}Zr_{0.5})B_2$ from the BHR powder (B3-1500-60m), which is very close to bulk HfB_2 and ZrB_2. The much lower hardness for sintered ceramics from the CTR powder is attributed to the higher porosity (see Figure 9A) as well as the presence of significant residual carbon (estimated to be ~8 wt.%!) in the CTR powder. Although carbon is often used as a sintering aid to help remove residual oxide for sintering of high temperature ceramics, the presence of large amount of excess carbon might be detrimental to the densification of the diboride solid solution.

The denser microstructure and higher hardness for the flash sintered $(Hf_{0.5}Zr_{0.5})B_2$ ceramic from the BHR powder suggest that the CTR powder, despite its phase purity in XRD, still needs further optimization, especially in terms of controlling residual amorphous carbon. On the other hand, although Figure 5 shows that $(Hf_{0.5}Zr_{0.5})B_2$ solid solution formed via the BHR method after 700ºC-6h low temperature heat treatment, the powder (B3-700-360m) was not yet suitable for flash sintering. This is because the powder, despite its nanograins, still contained significant amount of amorphous impurities. As mentioned in section 3.3.1, annealing at 1500ºC for 3 h in Argon led to 37.1% weight loss (and grain growth) for the powder. On the other hand, Figure S5 (B) shows the TGA-DSC for the B3-700-360m BHR powder after it was thoroughly washed. It lost 6.3% of weight at temperature below ~270°C. After that, the maximum weight gain of ~35% due to diboride oxidation was also lower than the expected value.

Finally, the thermal oxidation resistance in flowing air of the flash sintered bulk $(Hf_{0.5}Zr_{0.5})B_2$ samples was evaluated by TGA-DSC. Figure 10A shows the result for the sample from the CTR powder (C33-1500-60m). From room temperature to 600°C, there was no obvious weight change and no thermal feature. From ~600°C the weight started to increase, presumably due to the oxidation of the porous flash sintered diboride solid solution. This is consistent with the onset TGA oxidation temperature for the diboride solid solution powder (see Figure 8 and the related discussion). However, the weight gain appears to slow down slightly at ~850°C. This is attributed to the combined effect of the weight gain due to continued diboride oxidation and the *weight lost* due to oxidation of excess carbon in the CTR sample. Then, from ~900°C the weight gain accelerated again, presumably because all excess carbon was oxidized. Finally, the weight gain becomes really fast at ~1300°C, which is attributed to the active oxidation from $(Hf_{0.5}Zr_{0.5})B_2$ to (Hf, Zr)O_2 and B_2O_3 (the later starts to evaporate above ~800ºC) [22]. Overall, during the entire TGA process, heat flow was relatively featureless, and the total weight gain at ~1440°C was only 7.0%.

Figure 10B shows the TGA-DSC result for flash sintered $(Hf_{0.5}Zr_{0.5})B_2$ from the BHR powder. From ~800 to ~1000 °C, there was a very minor weight loss of ~0.5%. One possibility is that the flash sintered sample still contained some amorphous phases that evaporated in that temperature range. From ~1000 to 1440°C, there was a small weight gain of ~2.8%, which is attributed to onset of bulk oxidation for the diboride solid solution. The overall weight gain was much lower than the flash sintered sample using the CTR powder (~7% weight gain, see Figure 10A), which is consistent with the lower porosity and higher hardness for the flash sintered sample using the BHR powder.

4 | CONCLUSIONS

In this study, $(Hf_{1-x}Zr_x)B_2$ single phase solid solution powders with different Hf : Zr ratios were synthesized through two methods. The carbothermal reduction (CTR)-based method started from aqueous solution-based processing of $HfCl_4$, $ZrCl_4$, sucrose, and H_3BO_3 as the metal, carbon, and boron sources, respectively, followed by CTR reaction in Argon at high temperature (e.g., 1500°C). The borohydride reduction (BHR) method used $HfCl_4$ and $ZrCl_4$ to directly react with sodium borohydride ($NaBH_4$) at elevated temperature (e.g., 700 and 1500ºC) in Argon. For the CTR-based method, the formation of diboride solid solution was thermodynamically limited and only started to form from corresponding oxides at higher temperature (e.g., at 1320°C). For the BHR method, the diboride phase readily formed at much lower temperature (e.g., at 700°C). In addition, flash sintering (within ~5 min) of $(Hf_{0.5}Zr_{0.5})B_2$ powders synthesized through both the CTR-based and the BHR methods resulted in relative density of 70% and

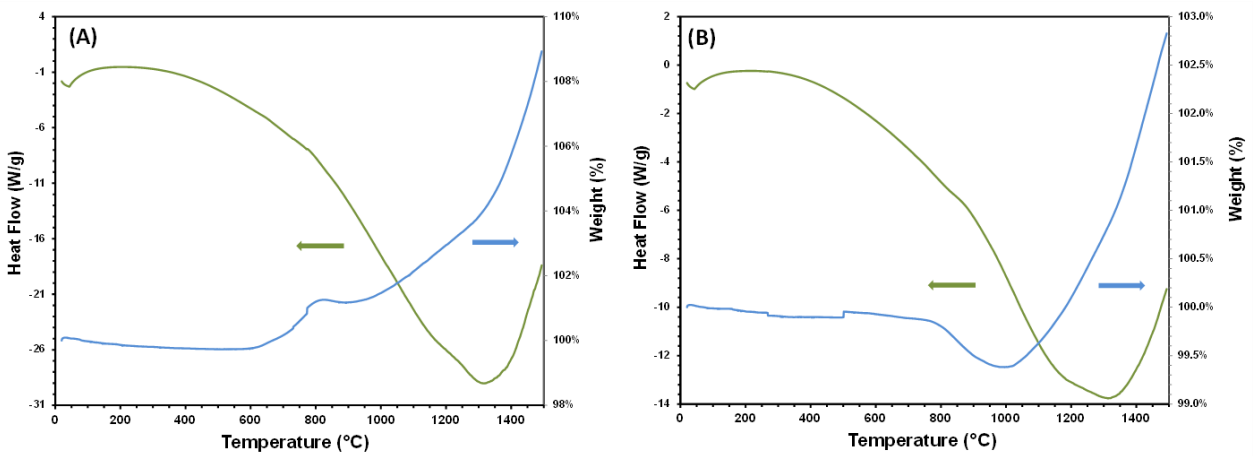

FIGURE 10 TGA and DSC profiles in air for bulk $(Hf_{0.5}Zr_{0.5})B_2$ prepared via flash sintering from (A) the CTR powder C33-1500-60m and (B) the BHR powder B3-1500-60m.

95%, respectively. The flash sintered $(Hf_{0.5}Zr_{0.5})B_2$ sample from the CTR powder had lower Vickers' hardness of ~8 GPa, while that from BHR powder was ~23 GPa, which is similar to bulk HfB_2 and ZrB_2. The difference is attributed to presence of significant residual carbon in the CTR powder that led to higher residual porosity. As to the oxidation resistance, the $(Hf_{0.5}Zr_{0.5})B_2$ powders from both the CTR-based and the BHR methods started to oxidize at ~700°C and completed at ~1000°C, while properly flash sintered bulk sample (from the BHR powder) displayed higher onset oxidation temperature of ~1000°C and much lower overall weight gain, consistent with the porosity of the sintered bodies.

Between the two synthesis routes, the CTR-based method starting from solution processing still needs much optimization as currently it tends to produce powders with significant residual carbon wrapping the diboride solid solution particles, while reducing carbon content in the starting recipes comes across challenges with oxide impurities. For the BHR method, the formation of non-carbon amorphous phase at lower temperature and the origin for Zr loss need to be better studied. In addition, understanding how to better control the microstructure of the synthesized powders is desirable, especially in terms of making the powders more uniform and reducing agglomerate formation. Finally, understanding the fundamentals including the defect evolution during the flash sintering process is also critical to future development of diboride ceramics for a broad range of applications.

5 | ACKNOWLEDGEMENT

The authors would like to thank Dr. Chunlei (Peggy) Wang of Florida International University for providing access to the Argon glove box for powder synthesis. The research was supported by the US Department of Energy (DOE) National Energy Technology Laboratory (NETL) Crosscutting Research Technology Program under Award Number DE-FE0026325.

REFERENCES

[1] W.G. Fahrenholtz, G.E. Hilmas, I.G. Talmy, J.A. Zaykoski, Refractory Diborides of Zirconium and Hafnium, Journal of the American Ceramic Society 90(5) (2007) 1347-1364.
[2] H.G. Fahrenholtz W, Ultra-High Temperature Ceramics - An Introduction to Ultra-High Temperature Ceramics, 2010.
[3] J.F. Justin, A. Jankowiak, Ultra High Temperature Ceramics : Densification, Properties and Thermal Stability, AerospaceLab (3) (2011).
[4] E. Wuchina, E. Opila, M. Opeka, W. Fahrenholtz, I. Talmy, UHTCs: Ultra-High Temperature Ceramic Materials for Extreme Environment Applications, Electrochem Soc Interface 16(4) (2007) 30.

[5] P. Foroughi, A. Rabiei Baboukani, A.F. Hernandez, C. Wang, Z. Cheng, Phase Control during Synthesis of Nanocrystalline Ultrahigh Temperature Tantalum-Hafnium Diboride Powders, Journal of the American Ceramic Society 101(12) (2018) 5745-5755.
[6] H. Wang, S.-H. Lee, L. Feng, The processing and properties of (Zr, Hf)B2–SiC nanostructured composites, Journal of the European Ceramic Society 34(15) (2014) 4105-4109.
[7] F. Monteverde, A. Bellosi, L. Scatteia, Ultra High Temperature Ceramics: Microstructure Control and Properties Improvement Related to Materials Design and Processing Procedures, Materials Science & Engineering A 485(1) (2008) 415-421.
[8] C. Zhang, B. Boesl, A. Agarwal, Oxidation resistance of tantalum carbide-hafnium carbide solid solutions under the extreme conditions of a plasma jet, Ceramics International 43(17) (2017) 14798-14806.
[9] C. Zhang, A. Loganathan, B. Boesl, A. Agarwal, Thermal Analysis of Tantalum Carbide-Hafnium Carbide Solid Solutions from Room Temperature to 1400 °C, Coatings 7(8) (2017) 111.
[10] R.G. Munro, Material properties of titanium diboride, Journal of research of the National Institute of Standards and Technology 105(5) (2000) 709-720.
[11] L.E. Pangilinan, C.L. Turner, G. Akopov, M. Anderson, R. Mohammadi, R.B. Kaner, Superhard Tungsten Diboride-Based Solid Solutions, Inorganic chemistry 57(24) (2018) 15305-15313.
[12] H. Wang, S.-H. Lee, H.-D. Kim, Nano-Hafnium Diboride Powders Synthesized Using a Spark Plasma Sintering Apparatus, Journal of the American Ceramic Society 95(5) (2012) 1493-1496.
[13] L. Chen, Y. Gu, L. Shi, Z. Yang, J. Ma, Y. Qian, Synthesis and oxidation of nanocrystalline HfB2, Journal of Alloys and Compounds 368(1) (2004) 353-356.
[14] L. Chen, Y. Gu, Z. Yang, L. Shi, J. Ma, Y. Qian, Preparation and some properties of nanocrystalline ZrB2 powders, Scripta Materialia 50(7) (2004) 959-961.
[15] M. Yu, S. Grasso, R. McKinnon, T. Saunders, M.J. Reece, Review of flash sintering: materials, mechanisms and modelling, Advances in Applied Ceramics 116(1) (2017) 24-60.
[16] S. Grasso, T. Saunders, H. Porwal, O. Cedillos-Barraza, D.D. Jayaseelan, W.E. Lee, M.J. Reece, Flash Spark Plasma Sintering (FSPS) of Pure ZrB2, Journal of the American Ceramic Society 97(8) (2014) 2405-2408.
[17] J. Zou, S. Grasso, L.-F. Liu, H.-B. Ma, M. Reece, J. Binner, Flash spark plasma sintering of HfB 2 ceramics without pre-sintering, Scripta Materialia 156 (2018) 115-119.
[18] P. Foroughi, C. Zhang, A. Agarwal, Z. Cheng, Controlling phase separation of TaxHf1−xC solid solution nanopowders during carbothermal reduction synthesis, Journal of the American Ceramic Society 100(11) (2017) 5056-5065.
[19] J.F.P. Xing, Low cost synthesis and fast sintering of nanocrystalline high entropy metal diboride ultra high temperature ceramic powders J. Xing NaBH4 high entropy boride 1 PF, 2018.
[20] S. Mondal, A. Durygin, V. Drozd, J. Belisario, Z. Cheng, Multicomponent bulk metal nitride (Nb 1/3 Ta 1/3 Ti 1/3)N 1− δ synthesis via reaction flash sintering and characterizations, Journal of the American Ceramic Society (2020).
[21] I. Barin, G. Platzki, Thermochemical Data of Pure Substances Third Edition, Two Volumes. Vol. 1: Ag-Kr and Vol. II: La-Zr By Ihsan Barin (ZEUS GmbH, FRG), in collaboration with Gregor Platzki. VCH: New York. 1995. 1900 pp. $535.00. ISBN 3-527-28745-0, 1996.
[22] T.A. Parthasarathy, R.A. Rapp, M. Opeka, R.J. Kerans, Effects of Phase Change and Oxygen Permeability in Oxide Scales on Oxidation Kinetics of ZrB.sub.2 and HfB.sub.2, Journal of the American Ceramic Society 92(5) (2009) 1079.
[23] C. Wang, M. Zinkevich, F. Aldinger, The Zirconia–Hafnia System: DTA Measurements and Thermodynamic Calculations, Journal of the American Ceramic Society 89(12) (2006) 3751-3758.
[24] Patnaik, Handbook of Inorganic Chemical Compounds, McGraw-Hill, NY, 2003.
[25] C. Peng, X. Gao, M. Wang, L. Wu, H. Tang, X. Li, Q. Zhang, Y. Ren, F. Zhang, Y. Wang, B. Zhang, B. Gao, Q. Zou, Y. Zhao, Q. Yang, D. Tian, H. Xiao, H. Gou, W. Yang, X. Bai, W.L. Mao, H.-k. Mao, Diffusion-controlled alloying of single-phase multi-principal transition metal carbides with high toughness and low thermal diffusivity, Applied Physics Letters 114(1) (2019) 11905.

[26] L. Zoli, P. Galizia, L. Silvestroni, D. Sciti, Synthesis of group IV and V metal diboride nanocrystals via borothermal reduction with sodium borohydride, Journal of the American Ceramic Society 101(6) (2018) 2627-2637.
[27] R.T.L.S.S.a.K. Takagi, Boride-Based Hard Materials, in: R. Riedel (Ed.), Handbook of Ceramic Hard Materials, Wiley-VCH, Weinheim, Germany, 2000, 2000, pp. 802– 945.

Science & Technology Transfer – No activities to transfer results for this project.

Presentations & Publications –

- On Dec 7th, 2020, the manuscript "Synthesis and flash sintering of $(Hf_{1-x}Zr_x)B_2$ solid solution fine powders" was accepted for publication at the *Journal of European Ceramic Society* (Article JECS13774, Manuscript ID JECS-D-20-01945R2 (2021)) that cover the major contribution of the research.
- On Nov 5th at 9:20-10:00 am, the PI presented the team and give an invited virtual presentation named "Synthesis and Flash Sintering of $(H_{f1-x}Zr_x)B_2$ Solid Solution Fine Powders" in the session of *Manufacturing and Processing of Advanced Ceramic Materials: Processing of Carbides, Borides, and Chlorides* in the conference of *2020 Materials Science & Technology (MS&T 20) held virtually*.

Inventions – There are no inventions or patents/patent disclosure made from this project

Appendix 1

Screen capture showing the manuscript "Synthesis and flash sintering of $(Hf_{1-x}Zr_x)B_2$ solid solution fine powders" has been accepted for publication for the ***Journal of European Ceramic Society (JECS)***

View Letter

Close

Date: 07 Dec 2020
To: "Zhe Cheng" chengzhe1978@hotmail.com;zhcheng@fiu.edu
From: "Journal of the European Ceramic Society" ees.elsevier@elsevier.com
Subject: Your Submission

Ms. Ref. No.: JECS-D-20-01945R2
Title: Synthesis and flash sintering of (Hf1-xZrx)B2 solid solution powders
Journal of the European Ceramic Society

Dear Professor Zhe Cheng,

I am pleased to inform you that your paper "Synthesis and flash sintering of (Hf1-xZrx)B2 solid solution powders" has been accepted for publication in the Journal of the European Ceramic Society.

Below are comments from the editor and reviewers.

Your accepted manuscript will now be transferred to our production department and work will begin on creation of the proof. If we need any additional information to create the proof, we will let you know. If not, you will be contacted again in the next few days with a request to approve the proof and to complete a number of online forms that are required for publication.

Thank you for submitting your work to the Journal of the European Ceramic Society.

Yours sincerely,

Laura Silvestroni
Editor
Journal of the European Ceramic Society

Comments from the editors and reviewers:

The authors addressed all issues in a satisfactory way.
Please correct the following sentece once you will receive the proofs:

Introduction, lines 36-39:
.....zirconium dioxide (ZrO2), i.e. the oxidation products of HfB2 and ZrB2, are porous and may become nonstoichiometric by forming oxygen vacancies....

%ATTACH_FOR_REVIEWER_DEEP_LINK INSTRUCTIONS%
****

****
For further assistance, please visit our customer support site at http://help.elsevier.com/app/answers/list/p/7923
Here you can search for solutions on a range of topics, find answers to frequently asked questions and learn more about EM via interactive tutorials. You will also find our 24/7 support contact details should you need any further assistance from one of our customer support representatives.

In compliance with data protection regulations, you may request that we remove your personal registration details at any time. (Use the following URL: https://www.editorialmanager.com/jecesoc/login.asp?a=r). Please contact the publication office if you have any questions.

Close

Supporting document for manuscript

FIGURE S1 Photo showing the graphite crucible with lid used for the heat treatment in synthesis of $(Hf_{1-x}Zr_x)B_2$ via either the CTR-based or the BHR methods. The graphite crucible has OD of 29.6 mm, ID of 22.0 mm, length of 38.8 mm. The crucible with lid helps reduce B_2O_3 evaporation and form diboride phase with higher purity (see also Figure S3B)

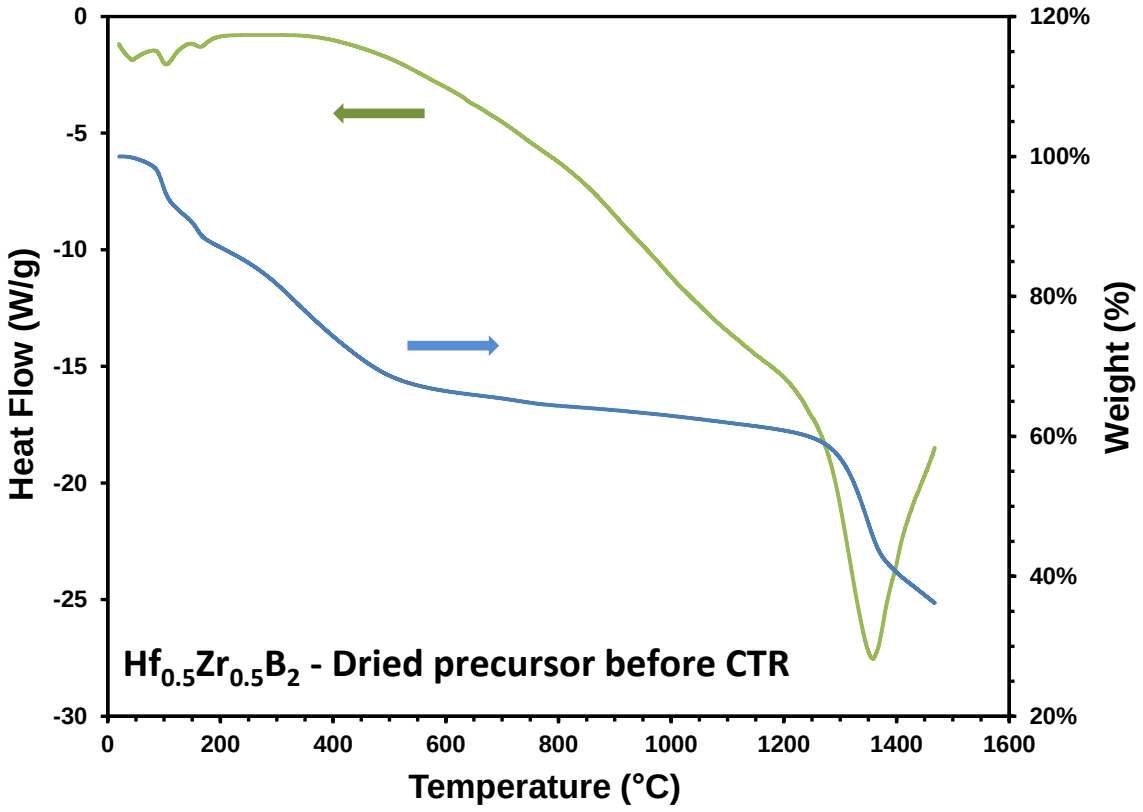

FIGURE S2 TGA and DSC curves in argon for the dried precursor from recipe C33 (starting Hf : Zr : B : C molar ratio = 0.5 : 0.5 : 3 : 10). The heating rate was 10°C/min. The weight loss before ~800°C is associated with loss of low molecular weight species (H_2O, CO, and others) due to dehydration and pyrolysis (thermal decomposition) processes to form carbon, B_2O_3, and (Hf, Zr)O_2, while the weight loss above ~1200°C is associated with the endothermic carbothermal reduction (CTR) reaction to form $(Hf_{0.5}Zr_{0.5})B_2$ as well as some B_2O_3 loss due to evaporation.

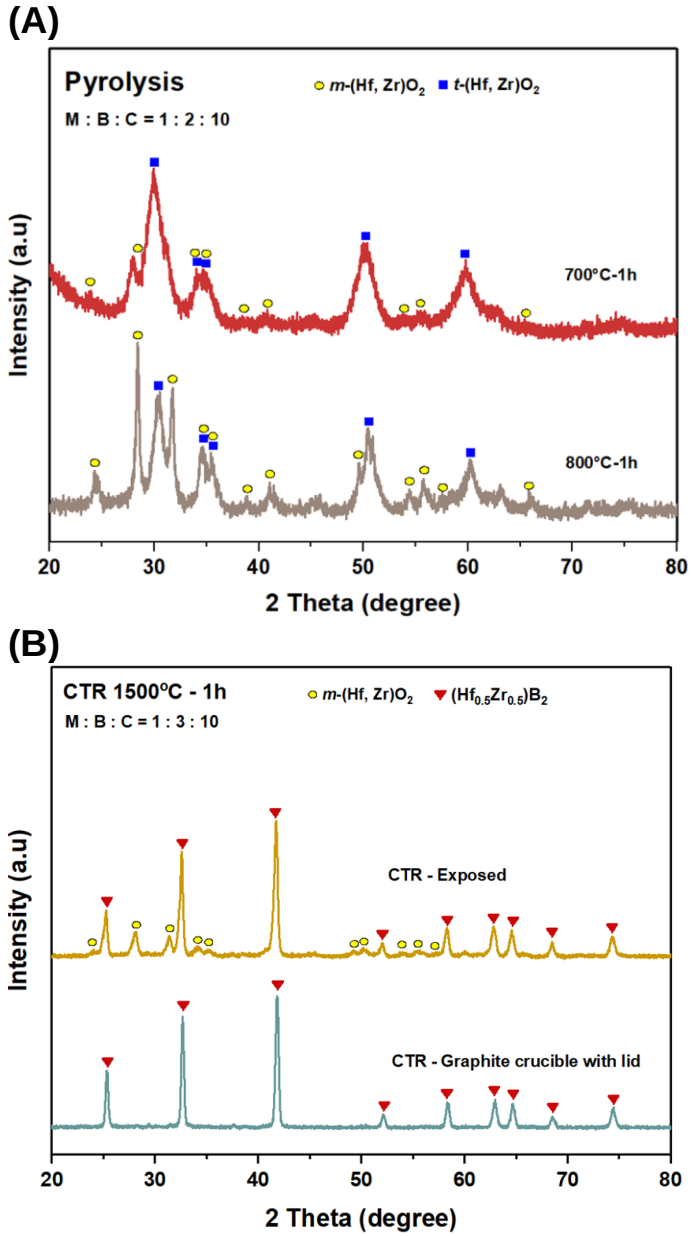

FIGURE S3. A, XRD for powders from recipe C31 (starting Hf : Zr : B : C molar ratio = 0.5 : 0.5 : 2 : 10) with final heat treatment 700 and 800°C for 1 h to show the effect of pyrolysis or thermal decomposition of the dried precursor. Note that after 700 or 800°C pyrolysis, (Hf, Zr)O_2 exists as a mixture of tetragonal and monoclinic phases, while B_2O_3 and carbon are amorphous. B, XRD for powders synthesized via the CTR-based method from recipe C33 (starting Hf : Zr : B : C molar ratio = 0.5 : 0.5 : 3 : 10) when the sample was either directly *exposed* to the Ar atmosphere (sample C33-1500-60m-E) or placed inside a graphite crucible with lid (sample C33-1500-60m) during the 1500°C-1h heat treatment. Note that the "exposed" sample gave significant amount of residual impurities such as monoclinic (Hf, Zr)O_2.

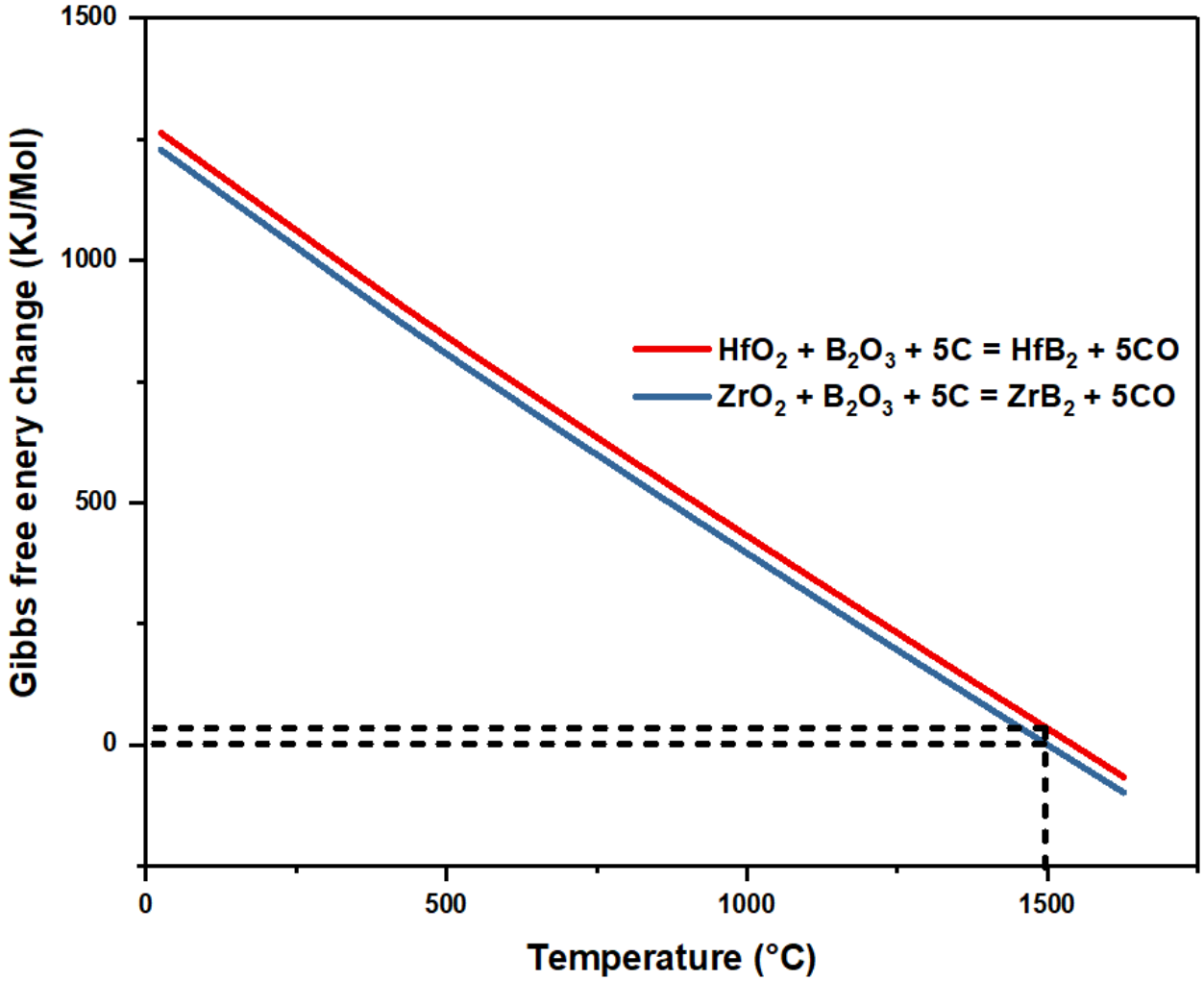

FIGURE S4 Calculated standard Gibbs free energy change ΔG^o as a function of temperature at the standard state (P_{CO} = 1 atm) for the formation of HfB_2 and ZrB_2 from carbothermal reduction (CTR) reactions.

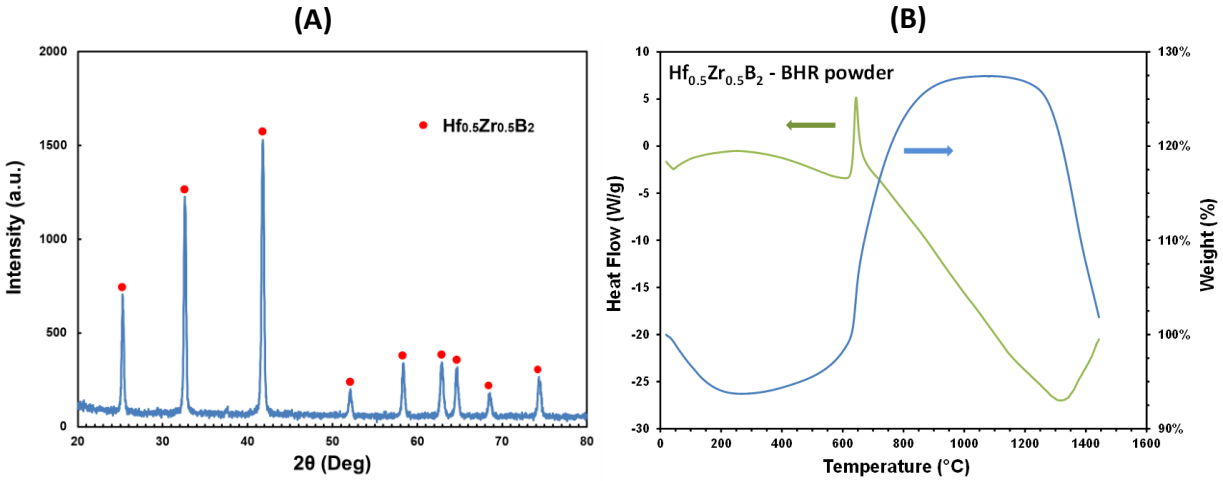

FIGURE S5 (A) XRD pattern for $(Hf_{0.5}Zr_{0.5})B_2$ solid solution powder B3-700-360m (synthesized at 700°C for 6 hours in Argon via the BHR method, see also Figure 5) *after* it was separately annealed at 1500°C for 3 hours in Argon. Note that after the 1500°C annealing, the XRD peak width became much smaller indicating grain growth, while the powder also lost 37.1% of its weight, presumably due to evaporation of amorphous Na-B compounds. (B) TGA and DSC curves in air for powder sample B3-700-360m. The TGA heating rate was 10°C/min. Note there is some weight loss at below ~200°C and the total weight gain at ~1000°C is much lower than the BHR powder synthesized at 1500°C for 1 h (see air TGA for sample B3-1500-60m in Figure 8B).

.

(A)

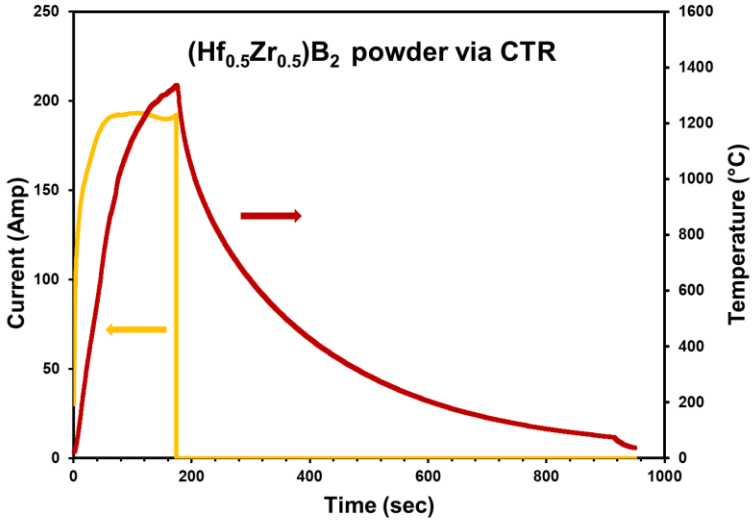

(B)

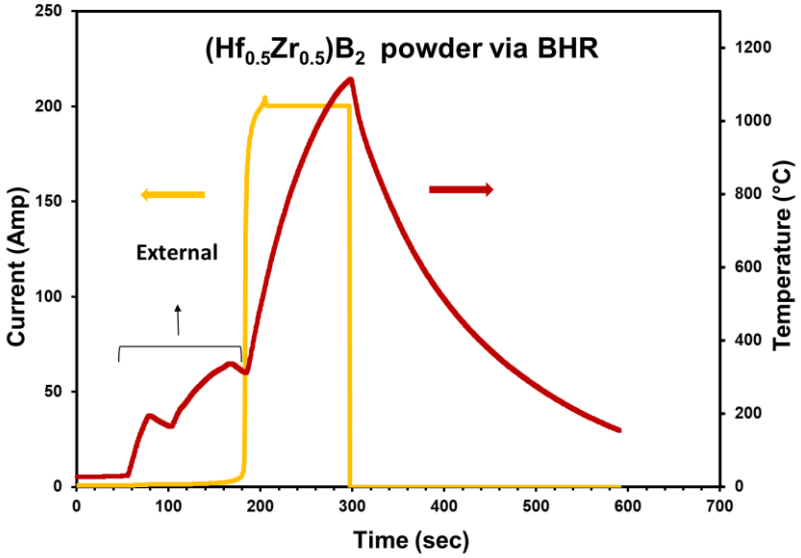

FIGURE S6 Plots of current and temperature vs time for flash sintering of $(Hf_{0.5}Zr_{0.5})B_2$ solid solution powders synthesized at 1500ºC-1h via (A) CTR and (B) BHR methods, respectively (sample ID C33-1500-60m and B3-1500-60m). Note that (i) 8 V DC was applied from time zero for both samples; (ii) external pre-heating was only applied for the BHR powder; (iii) the temperature shown in the plot is expected to be much lower (by several hundred or even a thousand degree Celsius) than sample's actual temperature because, due to instrument limitation, the thermocouple tip was at a distance away from the sample core and its position was not controlled with high precision (see reference [20] and section 3.4 of the main text for more details).

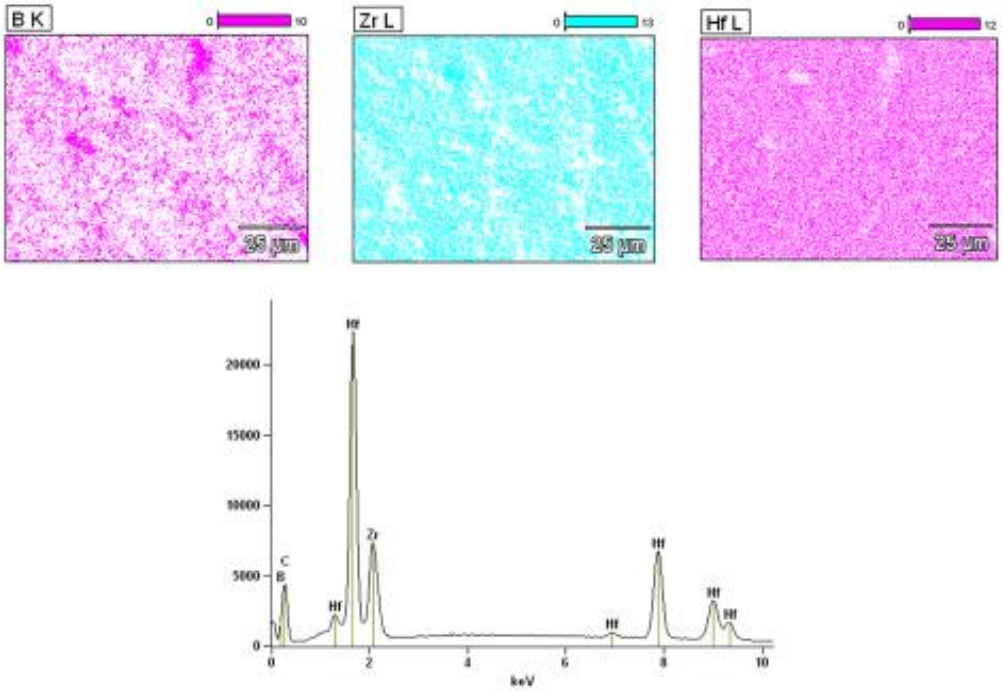

FIGURE S7 EDS mapping at magnification of 1000 and acceleration of 25.0 kV for flash sintered sample using CTR powder C33-1500-60m.

Appendix 2

Screen capture showing the presentation named "Synthesis and flash sintering of $(Hf_{1-x}Zr_x)B_2$ solid solution fine powders" given by the PI as an invited virtual presentation on Nov 5, 2020 at 9:20-10:00 am in the session of *Manufacturing and Processing of Advanced Ceramic Materials: Processing of Carbides, Borides, and Chlorides* in the *2020 Materials Science & Technology* (*MS&T 20*).

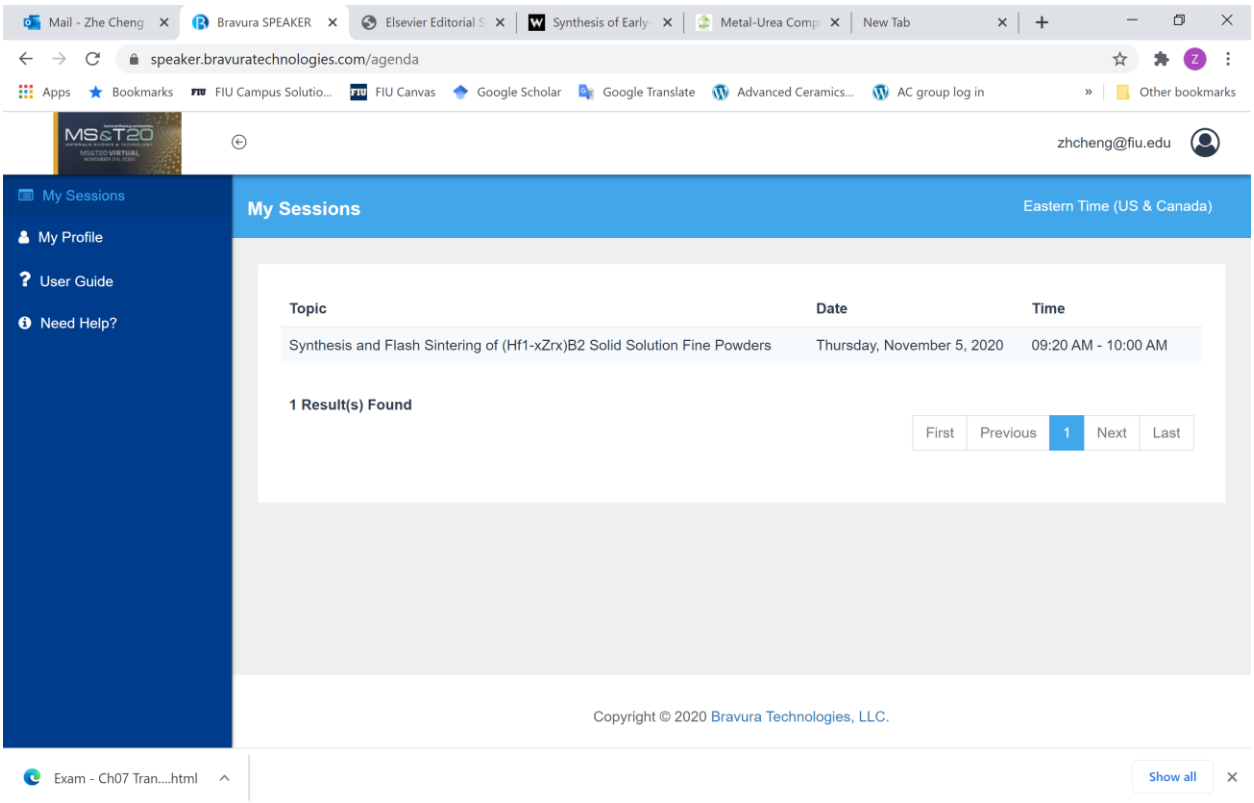

Synthesis and Flash Sintering of $(Hf_{1-x}Zr_x)B_2$ Solid Solution Fine Powders

Jose Belisario, Santanu Mondal, Iman Khakpour, Alexander Franco
Andriy Durygin, Zhe Cheng*
Department of Mechanical & Materials Engineering,
Florida International University, Miami, FL, U.S.A
zhcheng@fiu.edu

FLORIDA INTERNATIONAL UNIVERSITY

Diboride Ultra-high Temperature Ceramics

- ❑ ZrB_2 & HfB_2 UHTC
- ❑ Properties
  - ➢ T_m > ~3000 ℃
  - ➢ High hardness, electrical and thermal conductivity
  - ➢ Good thermal shock resistance
- ❑ Applications
  - ➢ Aerospace (e.g., rocket motor nozzle)

https://eandt.theiet.org/content/articles/2017/07/hypersonic-aircraft-move-closer-to-reality-with-revolutionary-ceramic-coating/

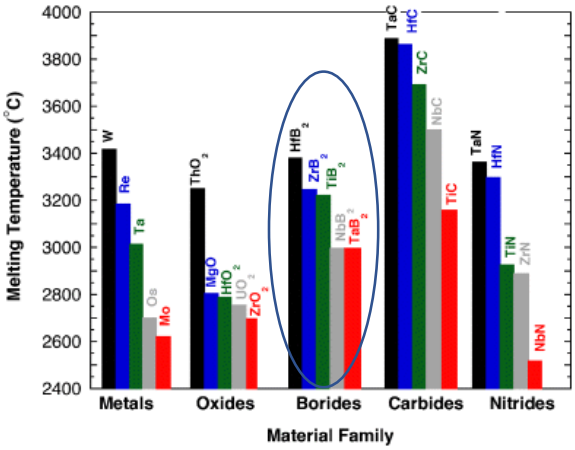

Melting temperature of selected materials

Fahrenholtz et al. Scripta Materialia, 2017, 129, 94

2

Motivation & Objectives

❑**Motivations**

- Alloying to form solid solutions might enhance properties for UHTC
- Not much work on diboride UHTC solid solution **fine powder synthesis** and **rapid sintering**

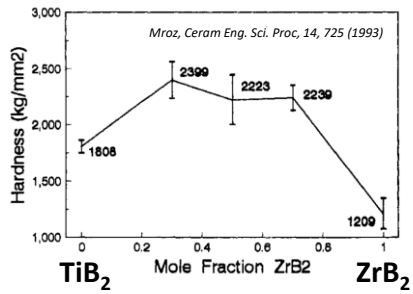

$(Hf\text{-}Zr)B_2$ Solid Solution

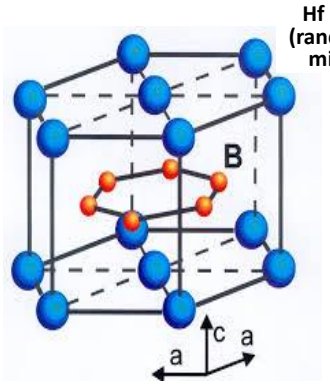

http://physics.aalto.fi/groups/nanospin/facilities/pulsed-laser-deposition/

❑**Objectives**

- Facile, low cost synthesis of $(Hf_{1-x}Zr_x)B_2$ solid solution fine powders via carbothermal reduction (CTR) and borohydride reduction (BHR) methods
- Rapid densification of $(Hf_{1-x}Zr_x)B_2$ by flash sintering

3

Synthesis via Solution Processing followed by CTR Reaction

❑ **Starting materials**

- Water soluble precursors

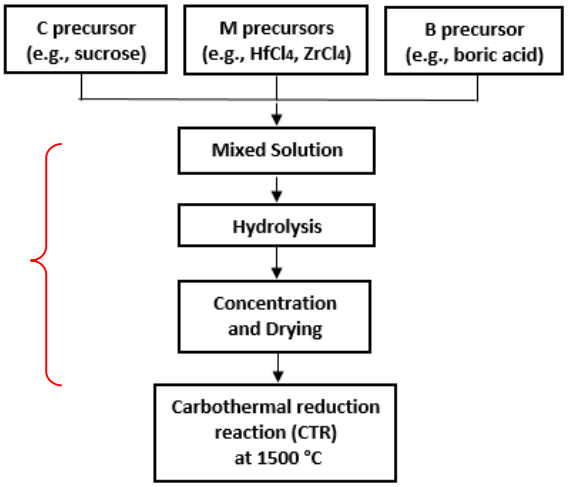

❑**Solution processing**

- $HfCl_4$, $ZrCl_4$ → $(Hf, Zr)O_2$
- Boric acid → B_2O_3
- Sucrose → C

❑**Heat treatment for CTR reaction**

$$Hf_{1-x}Zr_xO_2 + B_2O_3 + 5C = Hf_{1-x}Zr_xB_2 + 5CO$$

4

$(Hf_{0.5}Zr_{0.5})B_2$ Powder by CTR – High Temp Needed

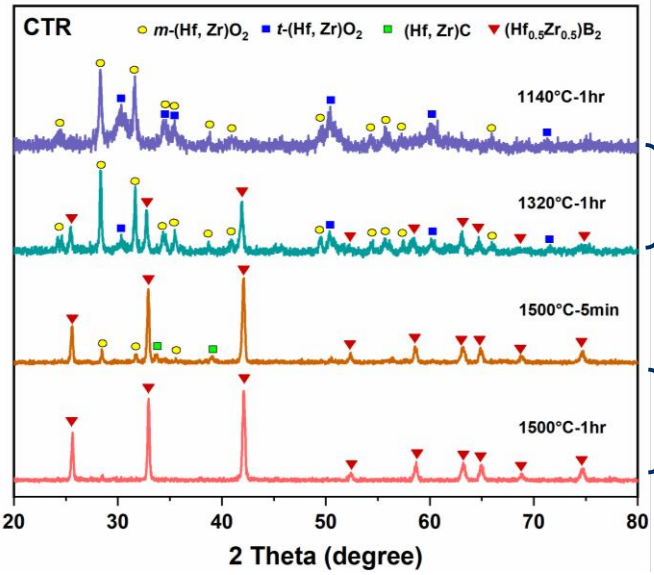

Starting molar ratio in solution:
Hf : Zr : B : C* = 0.5 : 0.5 : 3 : 10
* assuming 1 mol sucrose yields 12 mol C

Lower T → slow & incomplete reaction

Higher T → faster/complete reaction

Belisario et al., J European Ceramic Soc, under revision

5

$(Hf_{0.5}Zr_{0.5})B_2$ Powder by CTR – Excess B_2O_3 Needed

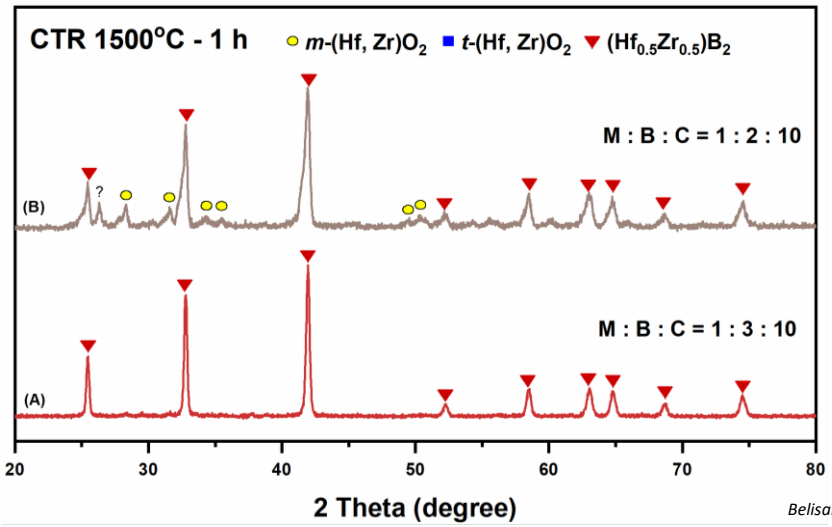

NO B_2O_3 excess

50% B_2O_3 excess

Belisario et al., J European Ceramic Soc, under revision

Excess boron (e.g., 50% access) needed to compensate for B_2O_3 evaporation

6

$(Hf_{1-x}Zr_x)B_2$ Powder by CTR – Varying Hf : Zr Ratio

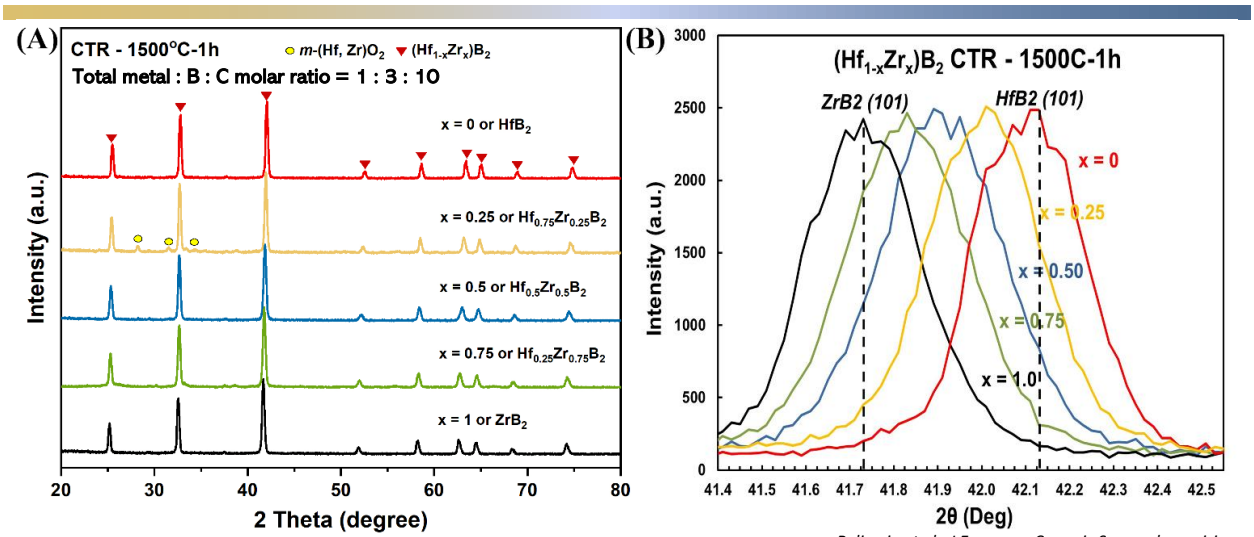

Belisario et al., J European Ceramic Soc, under revision

Gradual expansion of lattice parameter with increasing *x* or Zr, matching Vegards Law

7

CTR - Complication for *x* = 0.25 (Hf : Zr = 3 : 1) (1)

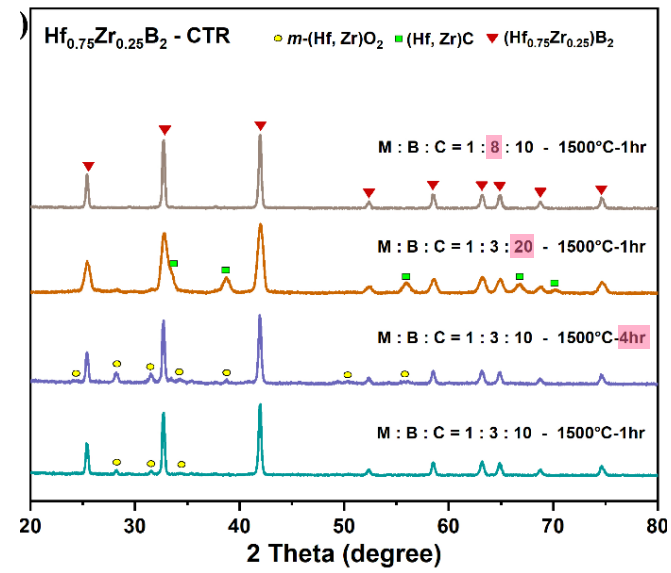

← More excess B_2O_3 removed $(Hf, Zr)O_2$

← More C removed oxides but left carbide!

← Longer CTR time did NOT remove oxides

← Persistent $(Hf, Zr)O_2$ after CTR for x = 0.25

Belisario et al., J European Ceramic Soc, under revision

8

CTR - Complication for x = 0.25 (Hf : Zr = 3 : 1) (2)

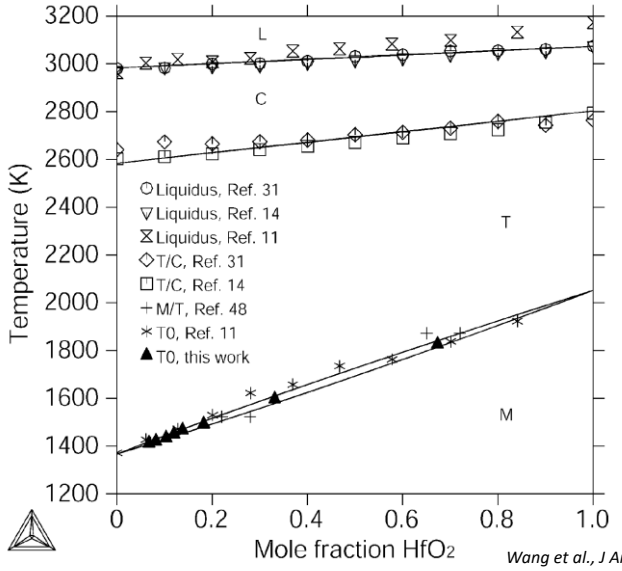

Wang et al., J American Ceramic Soc (2006) v89(12) 3751

Endothermic *m*-(Hf, Zr)O_2 → *t*-(Hf, Zr)O_2

- **Might compete with endothermic CTR and cause delay**
- **Allows time for more**
  - B_2O_3 evaporation
  - B_2O_3 (partial) reaction with C

} **residual (Hf, Zr)O_2**

9

$(Hf_{1-x}Zr_x)B_2$ Powder by CTR – Carbon Content Effects

Belisario et al., J European Ceramic Soc, under revision

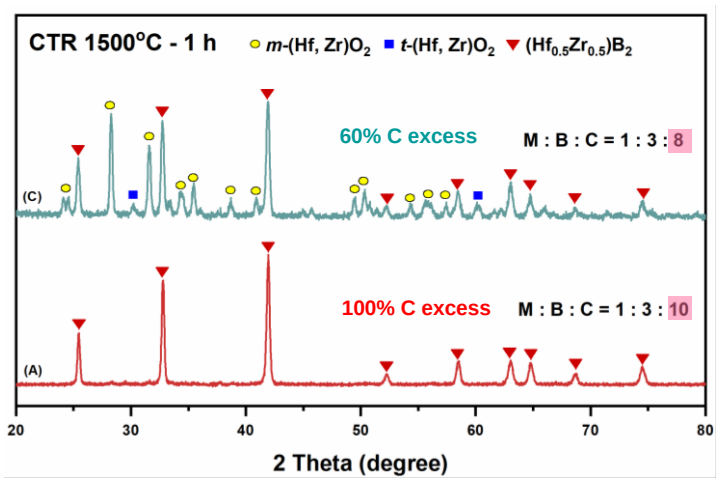

Low C excess prevents complete (Hf,Zr)O_2 removal

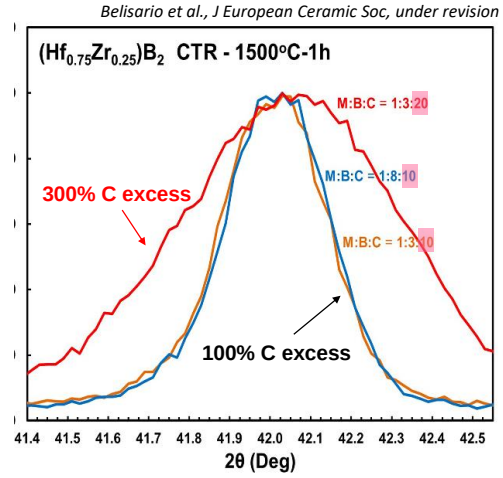

Too high C excess inhibits Hf & Zr inter-diffusion

10

Synthesis via Borohydride Reduction (BHR) Reaction

❑**Starting materials**

- Metal precursors
  - $HfCl_4$
  - $ZrCl_4$
- Boron source
  - $NaBH_4$

Mixing metal precursors (MCl_4) with $NaBH_4$

↓

Heat treat in a sealed graphite container (e.g., 1500 °C-1 h)

↓

Wash with water

❑**Example BHR reaction for Hf : Zr = 1 : 1**

$$HfCl_4 + ZrCl_4 + 4NaBH_4 = 2(Hf_{0.5}Zr_{0.5})B_2 + 4NaCl + 4HCl + 8H_2$$

11

$(Hf_{1-x}Zr_x)B_2$ Powder by <u>BHR</u> – Temperature Effect

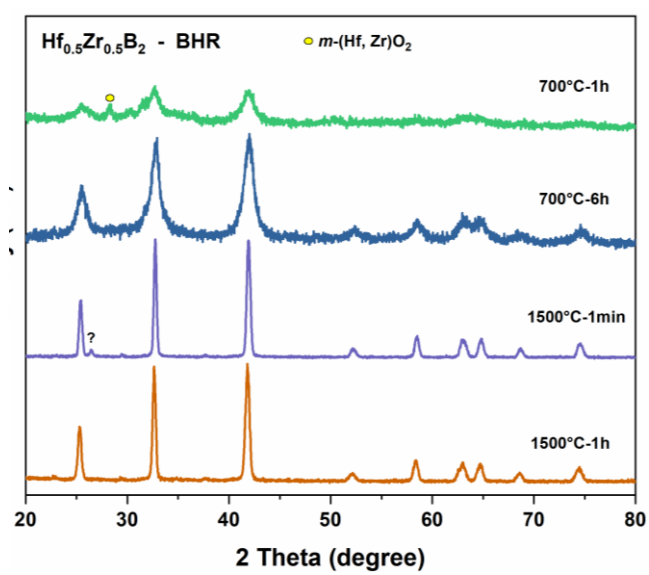

$HfCl_4 + ZrCl_4 + 4NaBH_4$ ➡ $2(Hf_{0.5}Zr_{0.5})B_2 + 4NaCl + 4HCl + 8H_2$

❑**BHR reaction occurs at T as low as 700°C!**

❑**Extremely fine grain at 700°C**

❑**Fast and complete reaction at 1500°C**

Belisario et al., J European Ceramic Soc, under revision

12

SEM for $(Hf_{0.5}Zr_{0.5})B_2$ Powder via <u>CTR</u>

Starting Hf : Zr : B : C = 0.5 : 0.5 : 3 : 10, 1500°C- 1 h in Ar

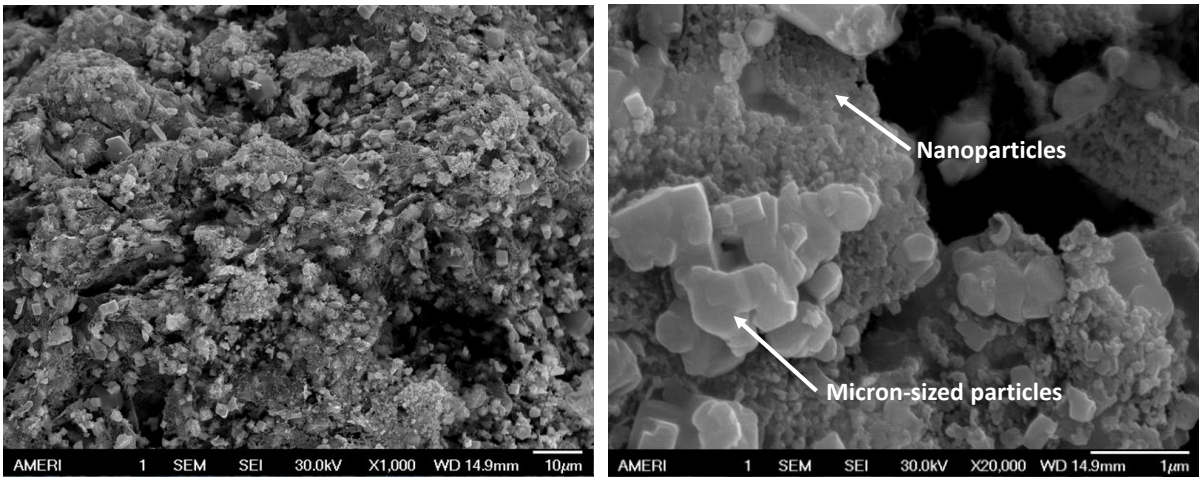

Belisario et al., J European Ceramic Soc, under revision

<u>Non-uniform</u> micron to nanoparticles

13

SEM for $(Hf_{0.5}Zr_{0.5})B_2$ Powder via <u>BHR</u>

Starting Hf : Zr : B = 0.5 : 0.5 : 3, 1500°C- 1 h in Ar

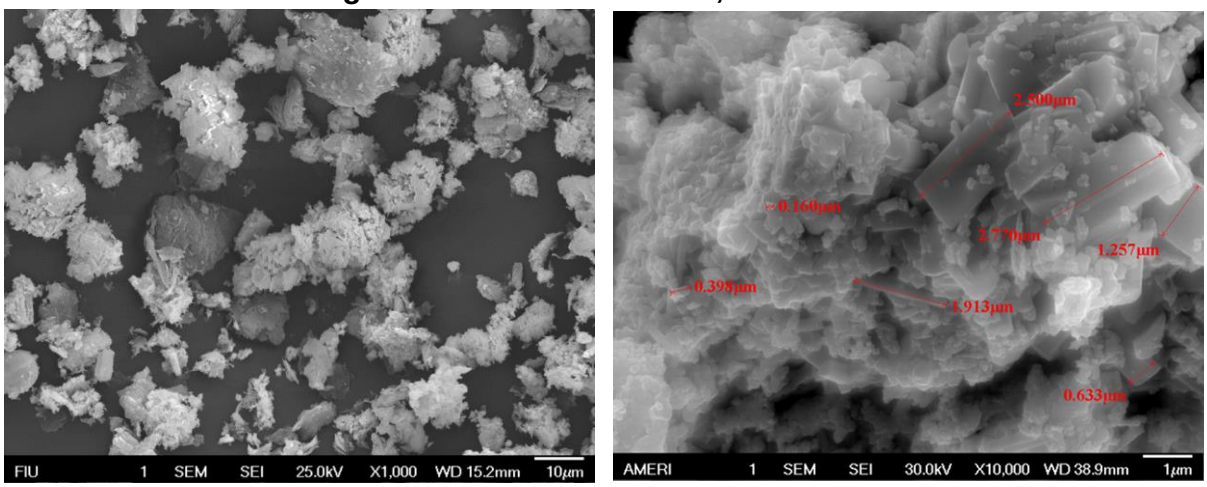

Belisario et al., J European Ceramic Soc, under revision

<u>Non-uniform</u> micron to submicron powders with thin and closely spaced platelets

14

TEM for $(Hf_{0.5}Zr_{0.5})B_2$ Powder via CTR

Starting Hf : Zr : B : C = 0.5 : 0.5 : 3 : 10, 1500°C- 1 h in Ar

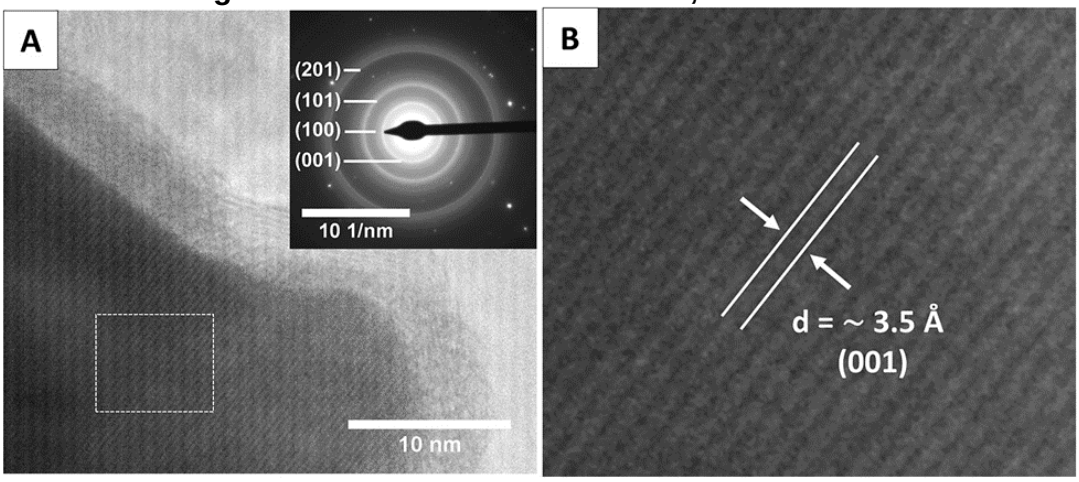

Belisario et al., J European Ceramic Soc, under revision

CTR $(Hf_{0.5}Zr_{0.5})B_2$ powder covered by amorphous carbon

15

TEM for $(Hf_{0.5}Zr_{0.5})B_2$ Powder via BHR

Starting Hf : Zr : B = 0.5 : 0.5 : 3, 700°C- 6 h in Ar

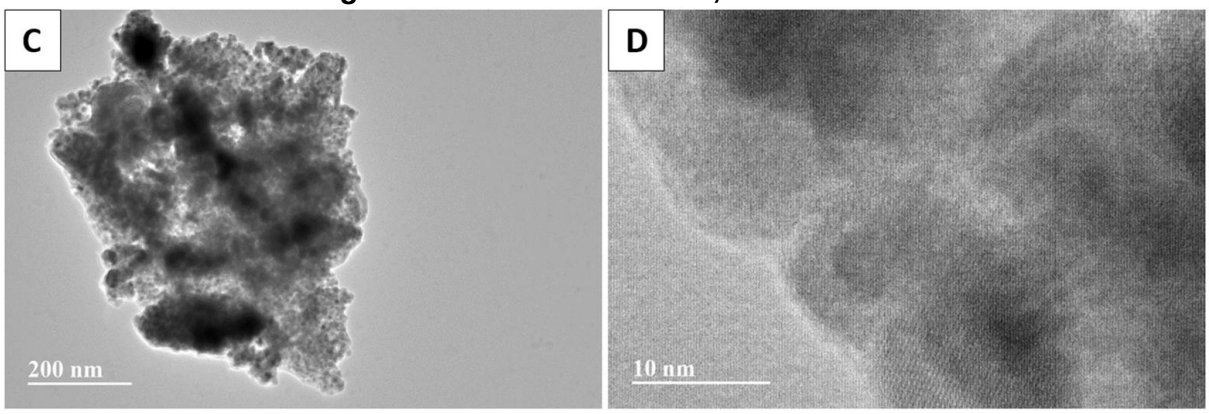

Belisario et al., J European Ceramic Soc, under revision

- **700°C-6 h BHR powder shows nano-grains, but are covered by amorphous, non- carbon phase**
- **Amorphous phase could be removed by subsequent 1500°C annealing in Argon, but with 37% weight loss**

16

TEM for $(Hf_{0.5}Zr_{0.5})B_2$ Powder via <u>BHR</u>

Starting Hf : Zr : B = 0.5 : 0.5 : 3, 700ºC- 6 h in Ar

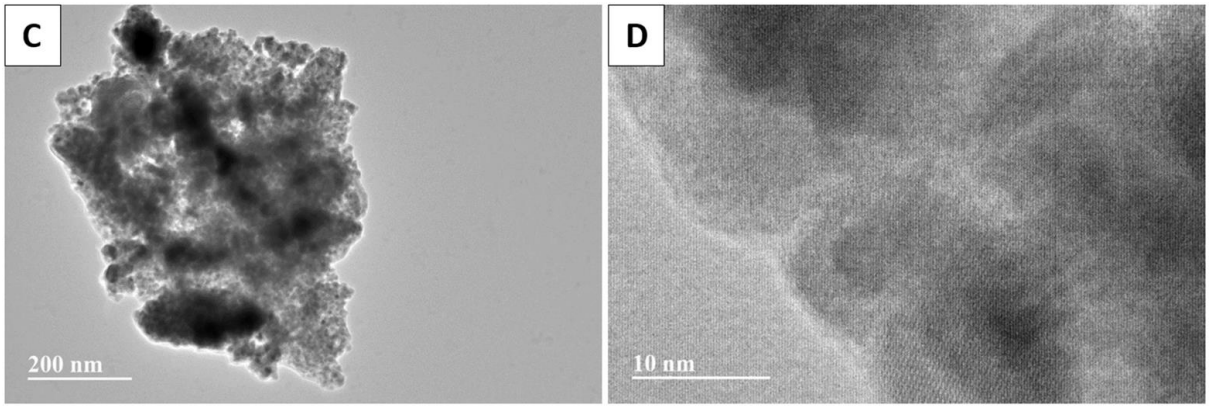

Belisario et al., J European Ceramic Soc, under revision

- ❑**700ºC-6 h BHR powder shows nano-grains, but are covered by amorphous, non- carbon phase**
- ❑**Amorphous phase could be removed by subsequent 1500ºC annealing in Argon, but with 37% weight loss**

16

Materials Densification via Flash Sintering

- ❑**Ceramics need sintering**
- ❑**Flash sintering**
  - ➢ Rapid densification (in min or even seconds) of powders with (DC) electrical current forced through the powder compact, accompanied by rapid decrease in sample resistance and increase in current and power dissipation
- ❑**Advantages**
  - ➢ Reduced temp, time, & energy
  - ➢ Finer microstructure
- ❑**Demonstrated systems**
  - ➢ 3 mol.% Y_2O_3-doped ZrO_2 (3YSZ)
  - ➢ Co_2MnO_4
  - ➢ Many more…

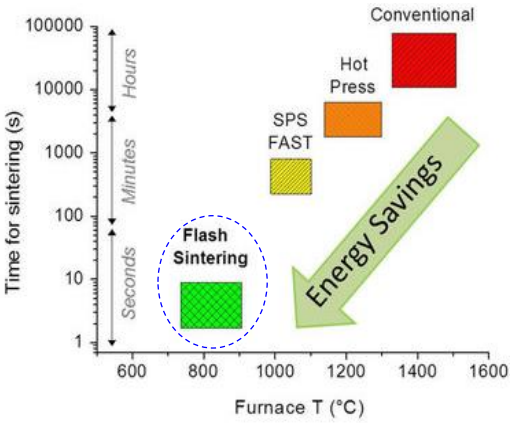

Cologna and Raj, J Am. Ceram. Soc (2010) 3556

18

In-House Sinter-Forging Type Flash Sintering Set-up

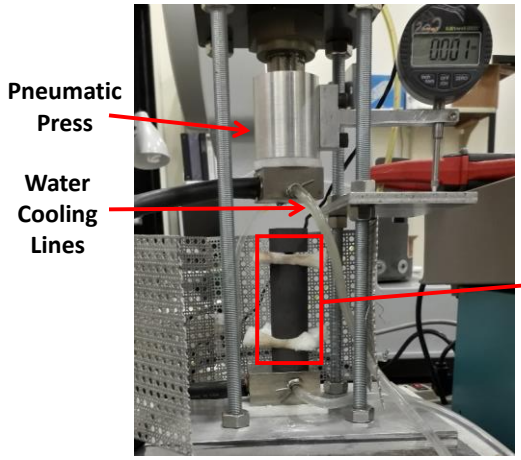

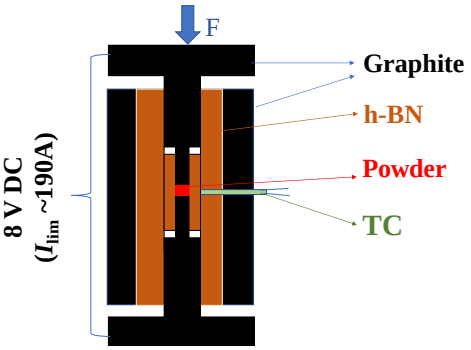

Sample after flash sintering

Mondal et al., J American Ceramic Soc (2020), v103(9), 4876
Belisario et al., J European Ceramic Soc, under revision

19

Current & Nominal Temperature during Flash Sintering

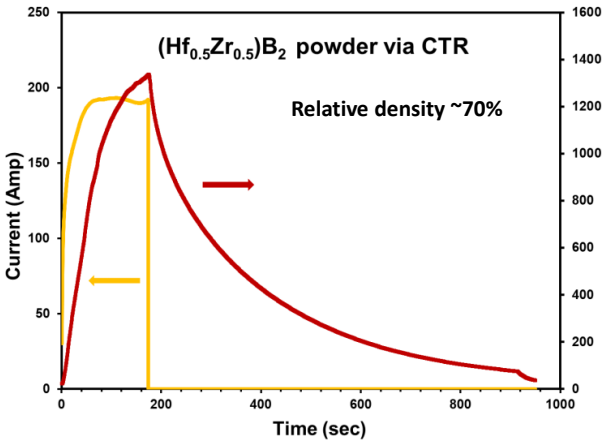

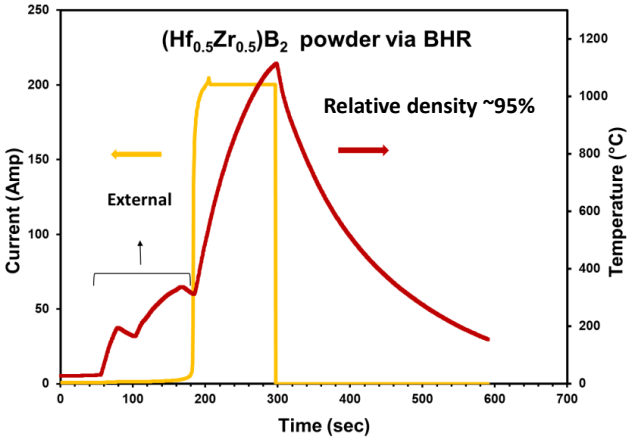

- ❑Preheating needed for BHR powder, but not for CTR powder
- ❑8 V constant DC → Rapid increase in current
- ❑FS finished in ~3-5 min

Belisario et al., J European Ceramic Soc, under revision

20

SEM for Flash Sintered $(Hf_{0.5}Zr_{0.5})B_2$ from <u>CTR</u> Powder

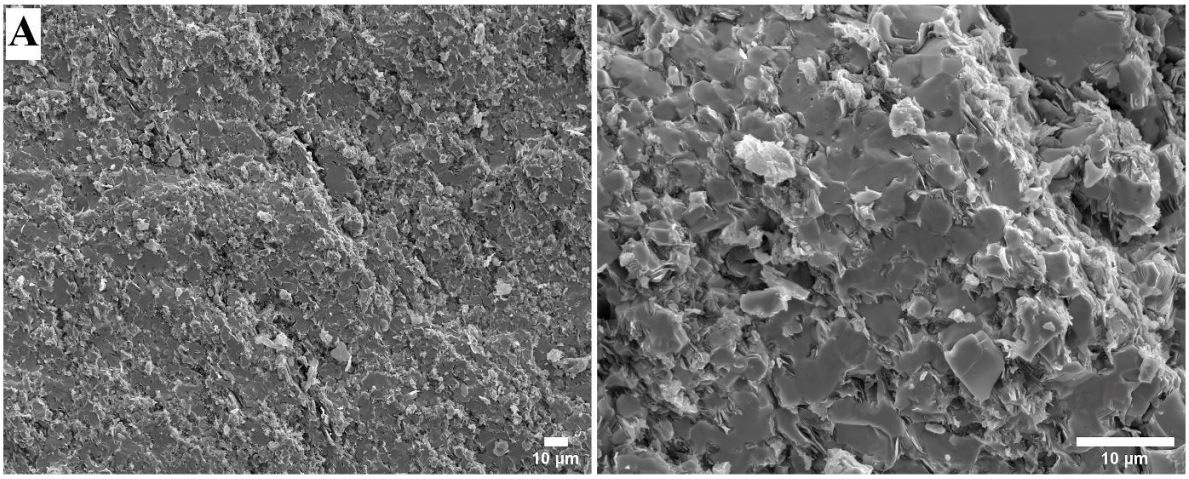

- ❑Two-phase structure showing layered structure from excess pyrolytic carbon
- ❑Significant residual porosity

Belisario et al., J European Ceramic Soc, under revision

21

SEM for Flash Sintered $(Hf_{0.5}Zr_{0.5})B_2$ from <u>BHR</u> Powder

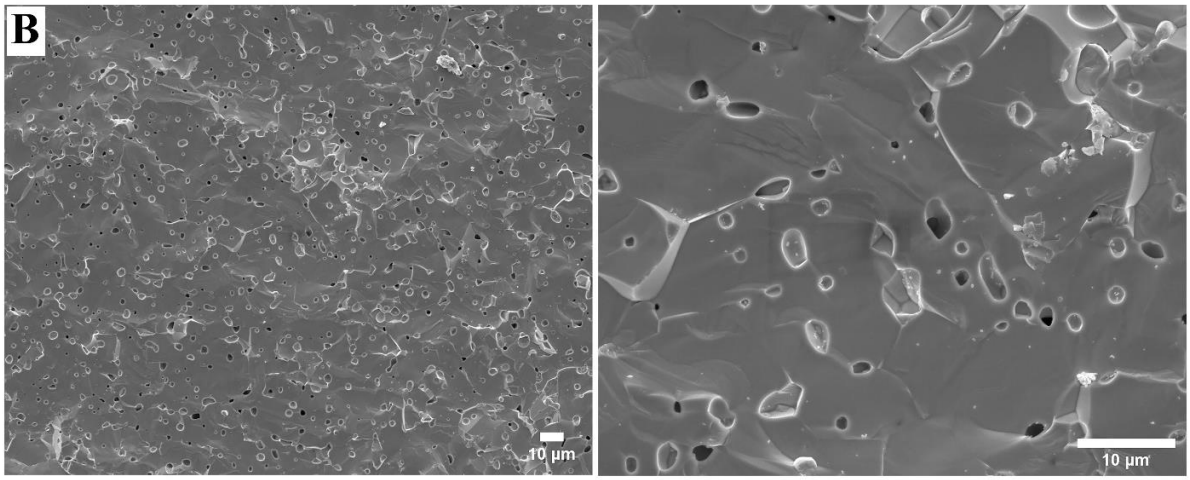

- ❑Dense structure with closed porosity
- ❑No secondary phases

Belisario et al., J European Ceramic Soc, under revision

22

EDS for Flash Sintered $(Hf_{0.5}Zr_{0.5})B_2$

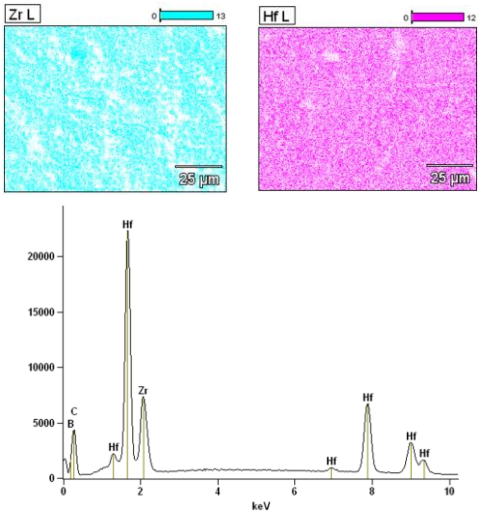

	Hf : Zr Atomic Ratio
CTR powder	1.01 ± 0.15
BHR powder	1.26 ± 0.31

- **Near stoichiometry ratio for CTR sample**
- **Hf : Zr ratio much higher than 1 : 1 for BHR sample**
  - $ZrCl_4$ sublimation due to boiling point (~331°C)?

- **EDS mapping shows uniform Zr & Hf distribution**

Belisario et al., J European Ceramic Soc, under revision

23

Hardness for Flash Sintered $(Hf_{0.5}Zr_{0.5})B_2$

- Flash sintered $(Hf_{0.5}Zr_{0.5})B_2$ from BHR powder gives hardness comparable to literature for HfB_2 & ZrB_2, and much higher than from CTR powder

	From CTR powder	From BHR powder	Literature HfB_2	Literature ZrB_2
Hardness (GPa)	8.2±0.1	23.0±0.4	21-22	27-28
Relative density	70%	95%		

- Higher hardness for flash sintered $(Hf_{0.5}Zr_{0.5})B_2$ from BHR powder than BHR is attributed to
  - lower porosity
  - Absence of excess carbon in the BHR powder

Belisario et al., J European Ceramic Soc, under revision

24

TGA in Air for Flash Sintered $(Hf_{0.5}Zr_{0.5})B_2$

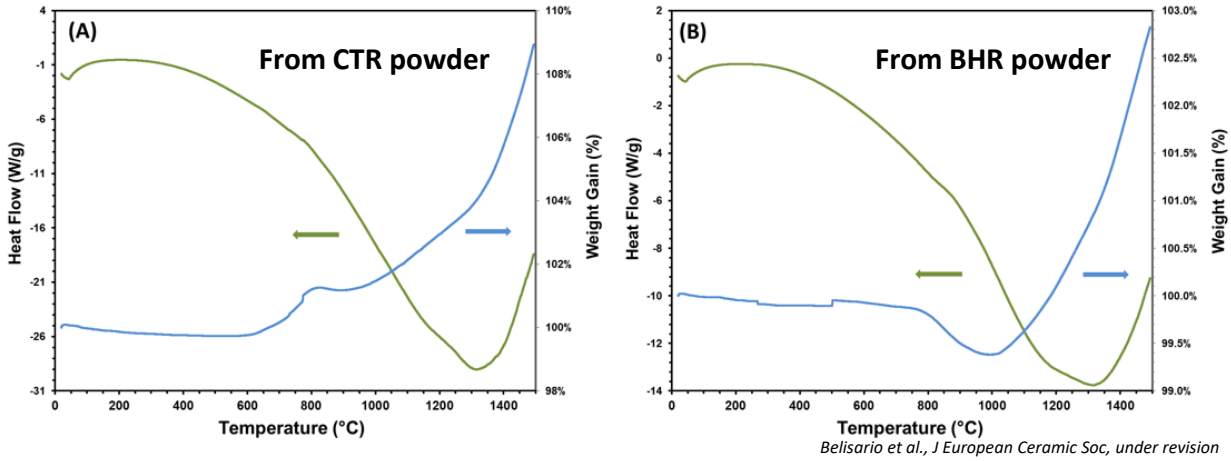

Belisario et al., J European Ceramic Soc, under revision

- Much lower overall weight gain for flash sintered $(Hf_{0.5}Zr_{0.5})B_2$ ceramics than for their powders
- Sample from BHR powder gives lower weight gain than from CTR due to lower porosity & lower excess carbon

25

Conclusions

- **Single phase** $(Hf_{1-x}Zr_x)B_2$ **solid solution powders** with varying Hf to Zr ratio were successfully synthesized via both carbothermal reduction (CTR)-based and borohydride reduction (BHR) methods
- Microstructure of powders synthesized showed **non-uniformity** with submicron to nano powders, sometimes with platelets morphology
- TGA oxidation of the diboride solid solution powders synthesized via CTR and BHR shows two-stage oxidation with similar onset temperature of ~700℃
- Flash sintering of $(Hf_{0.5}Zr_{0.5})B_2$ fine powders synthesized through both CTR and BHR methods were demonstrated. The BHR powder needs preheating for flash sintering, but delivers lower porosity and larger grains than from the CTR powder
- Hardness for flash sintered $(Hf_{0.5}Zr_{0.5})B_2$ from BHR powder is comparable to expectation, while the value from CTR powder is much lower. On the other hand, TGA oxidation in air show much lower total eight gain for flash sintered sample from BHR powder than from CTR method. Both these are attributed to the absence of excess carbon and lower porosity for the sample from BHR powder than from the CTR powder.

26